OPTICAL CROSS-CORRELATION STUDIES OF TWO-DIMENSIONAL PATTERNS

By

PAUL NORMAN HOWELL

Bachelor of Science
Oklahoma State University
Stillwater, Oklahoma
1959

Master of Science
Oklahoma State University
Stillwater, Oklahoma
1964

Submitted to the Faculty of the Graduate College
of the Oklahoma State University
in partial fulfillment of the requirements
for the Degree of
DOCTOR OF PHILOSOPHY
May, 1969

OPTICAL CROSS-CORRELATION STUDIES OF TWO-DIMENSIONAL PATTERNS

Thesis Approved:

Victor W. Bolie
Thesis Adviser

Samuel Silver

Paul A. McCollum

Jeanne Agnew

Karl M. Reid

A. O. Durham
Dean of the Graduate College

ACKNOWLEDGEMENTS

I wish to express my sincere gratitude to Professor Victor W. Bolie, chairman of my committee and thesis adviser, whose intense research interest in bionics and automata was instrumental in the selection of my thesis subject. For the many hours of his time he so generously devoted on my behalf and for his almost limitless patience, I am truly grateful.

I wish to thank Professor Harold T. Fristoe for serving as temporary chairman of my committee and for his guidance with my doctoral study plan. I wish also to express my appreciation to Professor Jeanne Agnew, Professor Paul McCollum, and Professor Karl Reid for their consenting to serve on my committee, for their advice and encouragement, and especially for their teaching excellence.

I am grateful to Mr. Dwayne Wilson for his help in securing the teaching assistantship, the Graduate College Summer Research Assistantship, and the Forgivable Loan from the Ford Foundation, which made the last two years of study financially possible. I am also grateful to Helen and Roy Helt for their generous help and advice with some of the photography problems, to Eldon Hardy for his promptness with the drafting, to Virginia Cook for the handwriting samples, and to Mrs. Claude Olvera for help with the proofreading.

I would also like to acknowledge the selfless devotion of my late wife, Dora. Her brave and cheerful attitude was a sustaining force to me throughout my graduate course work and has been an inspiration to me since.

TABLE OF CONTENTS

LIST OF FIGURES

CHAPTER I

INTRODUCTION

Analysis of two-dimensional optical patterns by automatic means is becoming of central importance in computerized analysis of large volumes of photographic information such as weather satellite records, machine interpretation of handwritten postal envelope addresses, automatic fingerprint identification and other similar tasks. Cross-correlation techniques appear to be promising in this regard both from theoretical and experimental points of view.

The purpose of this investigation is to examine in detail the possibilities of obtaining rapid two-dimensional cross-correlation functions between selected pairs of patterns by experimental means. Earlier studies have been made on the problem of optical cross correlation of two-dimensional patterns as well as other approaches to effecting or simulating pattern recognition systems.

Rosenblatt (1) gives several criteria to be applied to a simulation program. Under his "controls against trivial or ambiguous results" he mentions that the "actual form alone and not location on the retina or some other unintentional source of information" be considered. He describes a simplified version of known features of a mamalian vision system. The "Perceptron" has retinal points directly coupled to association cells. Each sensory point is connected to an "A" unit in either an excitory (+1) or inhibitory (-1) connection. Each "A" unit has fixed

threshold and delivers an output pulse if the algebraic sum of the inputs exceeds a given level. Each "A" unit is assigned a value which is adjustable during training such that during the test phase the total signal delivered by a set of the units approaches the desired signal. The total value distributed over all the units must remain constant according to an assumed constraint so that when one unit's value is increased all the other units' values are diminished.

Widrow and Hoff (2) describe a similar system which is implemented in the "Adaline" machine. This system used n adjustable weighting factors operating on n inputs to give an output. The desired output is forced by changing all weights by a fixed amount (positive or negative) stepwise to gradually reduce the error ϵ to zero. According to the authors, the process used will always converge. The authors set out to minimize the mean square error between the summation of the weighted outputs of the system and the desired output, showing that this criterion implies minimization of the average number of neuron errors (after quantization). The adaption amounts to a surface searching technique where a minimum is sought on an n-dimensional paraboloid. The experiments described consider a 3x3 field of sensors which are either excited or not. The field considered, unlike Rosenblatt's (1), assumes normalization of the pattern.

Steinbuch (3) describes a "learning matrix" and its two distinct operating phases. First, the learning phase requires a set of signals (properties or attributes) and a set of meanings (outputs) to be applied to the system simultaneously. The second phase (able phase) generates the output or meaning set according to a set of input signals. Implementation is said to be realizable from magnetic, electro-chemical or

electromechanical elements in the matrix.

Bolie (4) describes an algorithm whereby a machine may identify a particular symbol from an "alphabet" of signal vectors (assumed to be linearly independent.) The machine developes a matrix of column vectors representing the alphabet to be recognized. This matrix is inverted after the learning phase and then used to premultiply any vector to be identified. In the linearly independent, noiseless case the product is a unit vector in the symbol space. Various cases with noise are considered showing a deviation from the ideal unit vector results, but no serious recognition problem arises if a sufficient number of samples are considered during learning. This approach appears significant in the information retained since no quantization occurs internal to the process.

Eden (5), and Mermelstein and Eden (6) use a model for stroke generation in handwriting analysis which considers any stroke to be representable by two pairs of quarter-wave sinusoidal segments, one for each of the horizontal and vertical components during the vertically accelerating and decelerating sections, respectively. From these segments a parameter vector is formed including such characteristics as displacement, curvature, pen velocity, amplitude, etc. The authors chose the lower case Latin alphabet and represent the 26 letters by 52 different symbols plus a null stroke. A set of allowable sequences is used along with probabilities of their occurrence to expedite the search procedure. When each subject's writing was in the learned ensemble, results seemed reasonable; if not, the error rate was very high. If the subject's writing was the only sample used, the results were excellent, that is, the error rate was reduced to about that of a human reader.

Blackwell (7) summarizes a group of "neural" theories of visual discrimination and compares them to the physical quantum theory groups. Much attention is given to the quotient $\Delta I/I$ (change in intensity divided by intensity). Evidence of a 5-6 cps scanning mechanism is given as well as a discussion of the position of the stimulus in the visual field. A time delay storage mechanism is also discussed. The bulk of the paper deals with threshold measurements and the validation of the measurement methods.

Kazmierczak and Steinbuch (8) feel that the human visual system should be considered in designing perception systems and compare some properties of the human visual system with existing mechanical perceptual systems. They describe the necessity to select a set of features independent of changes in registration, skew, size, contrast, deformation, etc. They note the evidence of data reduction from the 10^8 nerve fibres in the human optic nerve; in addition, abstraction ability and imagination indicate that some feedback must exist. The learning matrix described here consists of column inputs (a feature vector) and row outputs (the category) connected with variable weights as conventionally used in adaptive network schemes. The weights may be positive or negative as may be the features x_j which are assumed to be analog in character. The authors give comparative examples in two dimensions for separating the pattern set aggregation. Throughout their paper the need for schemes of feature abstraction is emphasized.

Cutrona, et al (9), Montgomery and Broome (10), and Vander Lugt (11) have presented mathematical theories of spatial filtering of optical patterns in which both the amplitude and the phase relationships of the pattern-transmitting light beam are considered as essential parts of the

pattern. Montgomery and Broome (10) present considerable filter theory extended to two dimensions and computer simulation experiments. Cutrona, et al (9) present techniques of both spatial and "frequency domain" filtering and suggest the necessary optics for achieving the filtering action in one or two dimensions. Vander Lugt (11) extends the spatial filtering theory to include non-uniform noise distributions where a prior knowledge of the noise function is known. Experiments described in the latter two papers require a coherent light source to establish phase relationships of the light throughout the optical system. This theory is the basis of the more modern laser-projected hologram patterns.

An excellent survey of many different commercial approaches to mechanized automatic recognition of standardized letters, numbers and punctuation marks has been presented by Falk (12).

McLachlan (13) extends optical correlation techniques developed in earlier work (14) toward the problem of pattern recognition. One and two dimensional convolutions are performed using masks, light and photocell. The level registered on the photocell is recorded versus the position to yield the correlation function. Although examples are shown of characters of different sizes, both size and orientation seem to be requisite for meaningful correlations in one or two dimensions.

A method for obtaining the autocorrelation of any image directly using only one photographic plate and a combination of lens, mirror and beam splitter is described by Kovasznay and Arman (15). The authors also note some of their observations on the autocorrelation of randomly positioned ensembles of simple patterns. Meyer-Eppler and Darius (16) describe a two plate correlator on which cross-correlation can be made. A matrix of cross-correlation patterns for five upper-case alphabet

letters was presented with comments on the various types of symmetry observed in the resulting patterns.

Comprehensive treatments of the present state of knowledge of the detailed functions of the central nervous system and of the optic tracts may be found in the relatively recent compilations of Gerrard and Duyff (17), Wiener and Schade (18), Reiss (19), and Wiener and Schade (20).

Convincing evidence is presented by the authors cited and others that when a suitable set of parameters or features exist, various methods may be employed to effect a pattern recognition system. Extensive work applicable to machine printed symbols has been done on the basis of a 3x3 field of sensors as assumed by Widrow and Hoff (2) and others. While Eden (5) considers the problem of handwriting on a real-time or tracking basis, none of these reports have been devoted to feature abstraction in off-line analysis of handwriting and similar two-dimensional patterns. It is the apparent need for such feature abstraction techniques that motivates this study.

Following this introduction and overview of the literature is an examination of the theory of two-dimensional cross correlation and the development of a resultant theorem. Presented thereafter are details of the design and construction of the laboratory equipment used for the investigation. Details in support of experimental verification of theoretical predictions are then presented, following which are the results of studies made with certain specialized two-dimensional patterns.

CHAPTER II

OPTICAL CROSS-CORRELATION THEOREM

Correlation techniques seem to hold much promise in the problem of two dimensional pattern recognition. Point by point measurement of the correlation function of two dimensional patterns has proved to be quite laborious, however, since small increments of displacement in two dimensions make many measurements necessary. The optical method described here allows the entire correlation function to be obtained at once in the form of a light intensity distribution on a plane.

The principles of the optical method of producing two dimensional pattern correlations can be outlined with reference to Figure 1. The planar diffused light source is ideally a plane in which every elemental area emits light in all directions, with a normalized flux intensity of unity everywhere in the 4π steradians surrounding the elemental area. Light rays emanating from some of the points in this planar diffused light source travel through the clear regions of transparencies A and B and impinge on the observation plane C.

The first transparency (plane A) contains aligned and centered coordinates x_1, y_1. The pattern in plane A is defined by the transparency function $f(x_1, y_1)$ which varies from a value of zero for complete opacity to a value of unity for complete transparency.

The second transparency (plane B) contains similarly aligned and

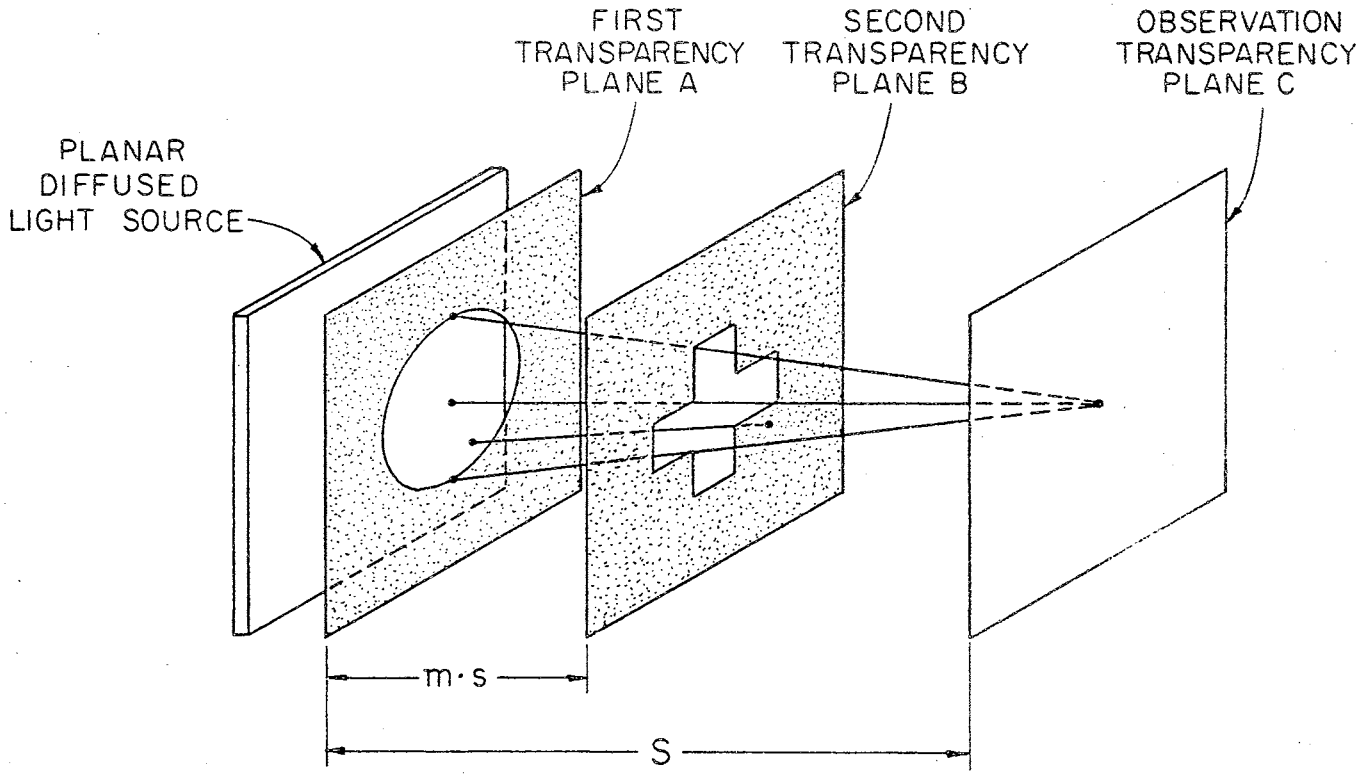

Figure 1. General Geometry of Optical Cross-Correlation Process

centered coordinates x_2, y_2. The pattern in plane B is defined by the transparency function $g(x_2, y_2)$ which varies from a value of zero for complete opacity to a value of unity for complete transparency. It is assumed that the light is attenuated but not refracted or scattered by the pattern $g(x_2, y_2)$.

The observation or detection plane (C), which might be a "frosted-glass" viewing surface, contains aligned and centered coordinates α and β. The observed pattern in plane C is defined by the detected light intensity function $h(\alpha, \beta)$, which increases from a value of zero for no light-ray impingement to increasingly more positive values for brighter illumination. It will be assumed that over the area of interest in the observation or detection plane (C) the effects of the inverse square law and cosine variations are insignificant.

A mathematical analysis of two dimensional pattern correlation by the optical method illustrated in Figure 1 can be initiated with the aid of some mathematical definitions. The optical processes of both magnification and reduction of images must be considered.

DEFINITION 1: An image function is defined as a light intensity variable $G(\theta, \omega)$ expressed as a function of two orthogonal coordinate variables θ and ω.

DEFINITION 2: A k-stretched image function is defined as the function obtained by replacing the coordinate variables θ and ω of an original or parent function $G(\theta, \omega)$ with $k\theta$ and $k\omega$, respectively, where k is an omnidirectional stretching factor.

In order to illustrate the idea of a k-stretched image function in relation to its parent image function, let $G(\theta, \omega)$ be an image func-

tion as defined earlier, and specifically

$$G(\theta, \omega) = \begin{cases} 1 & , |\theta| \leq 2 \text{ and } |\omega| \leq 3 \\ 0 & , \quad \text{elsewhere.} \end{cases} \tag{2-1}$$

Let $F(\theta, \omega) = G(k\theta, k\omega)$, i.e. $F(\theta, \omega)$ is the k-stretched image function whose parent image is $G(\theta, \omega)$. Then

$$G(k\theta, k\omega) = \begin{cases} 1 & , |k\theta| \leq 2 \text{ and } |k\omega| \leq 3 \\ 0 & , \quad \text{elsewhere.} \end{cases} \tag{2-2}$$

Alternatively

$$F(\theta, \omega) = \begin{cases} 1 & , \left|\frac{\theta}{k}\right| \leq 2 \text{ and } \left|\frac{\omega}{k}\right| \leq 3 \\ 0 & \quad \text{elsewhere.} \end{cases} \tag{2-3}$$

Referring to the functions described by Equations (2-1) and (2-3), and to Figure 2, it will be seen that when $k > 1$ the pattern represented by the k-stretched image function is physically smaller than the pattern represented by the parent image function. On the other hand, for $k < 1$ the pattern represented by the k-stretched image function is physically larger than the pattern represented by the original or parent image function, as illustrated in Figure 3.

The detected light intensity in a neighborhood of the point (α, β) on plane C of Figure 1 is comprised of a summation of the effects of all of the light sources whose rays are transmitted by incremental openings or transparencies in planes A and B as suggested in the one-dimensional representation shown in Figure 4. Plane C is separated by the distance s from plane A, and plane B is located at the intermediate distance ms from plane A where $0 < m < 1$. The geometry of Figure 4 shows that a

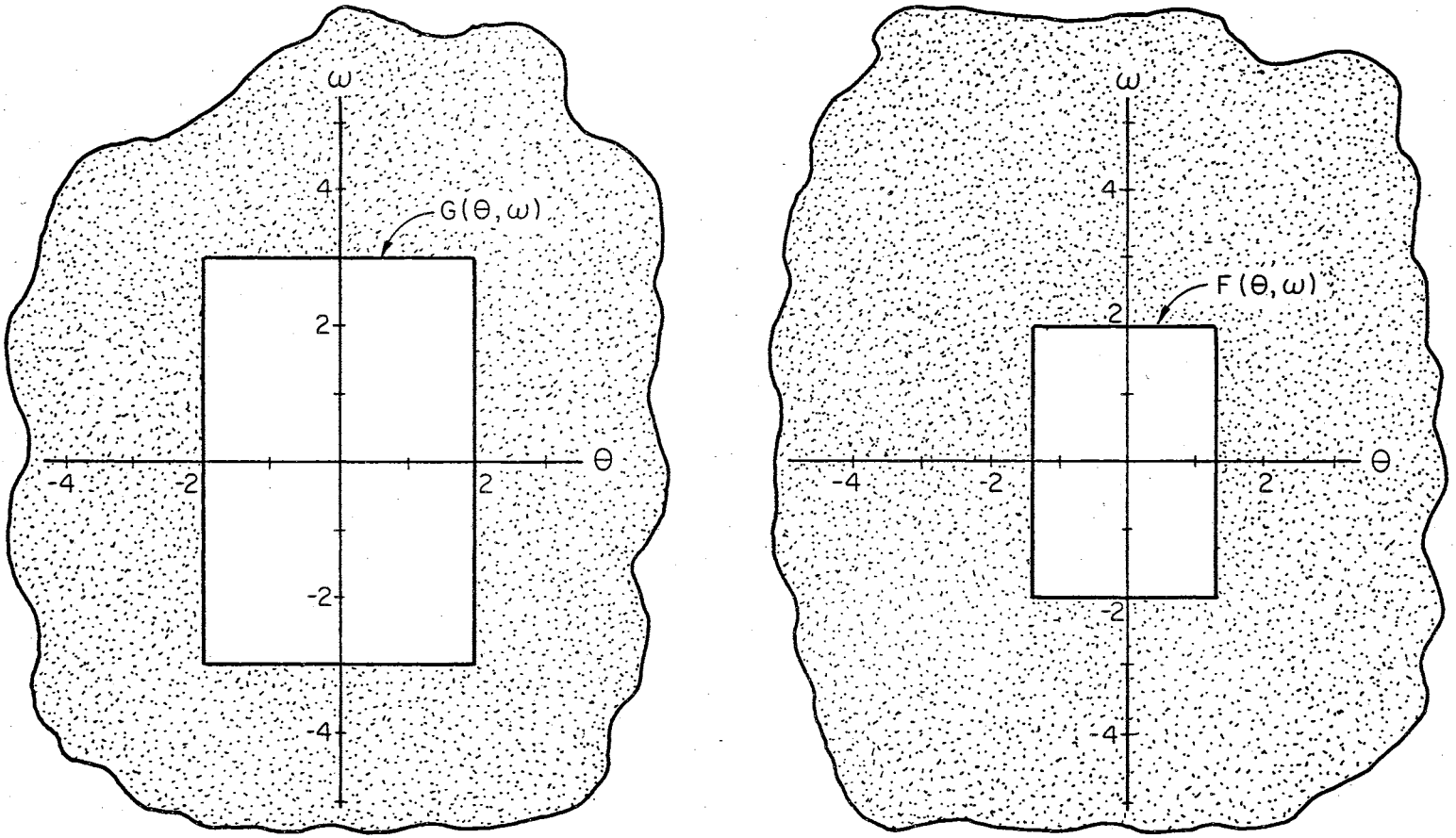

Figure 2. Example of Parent Image Function (Left) and K-Stretched Image Function (Right) for K=1.5

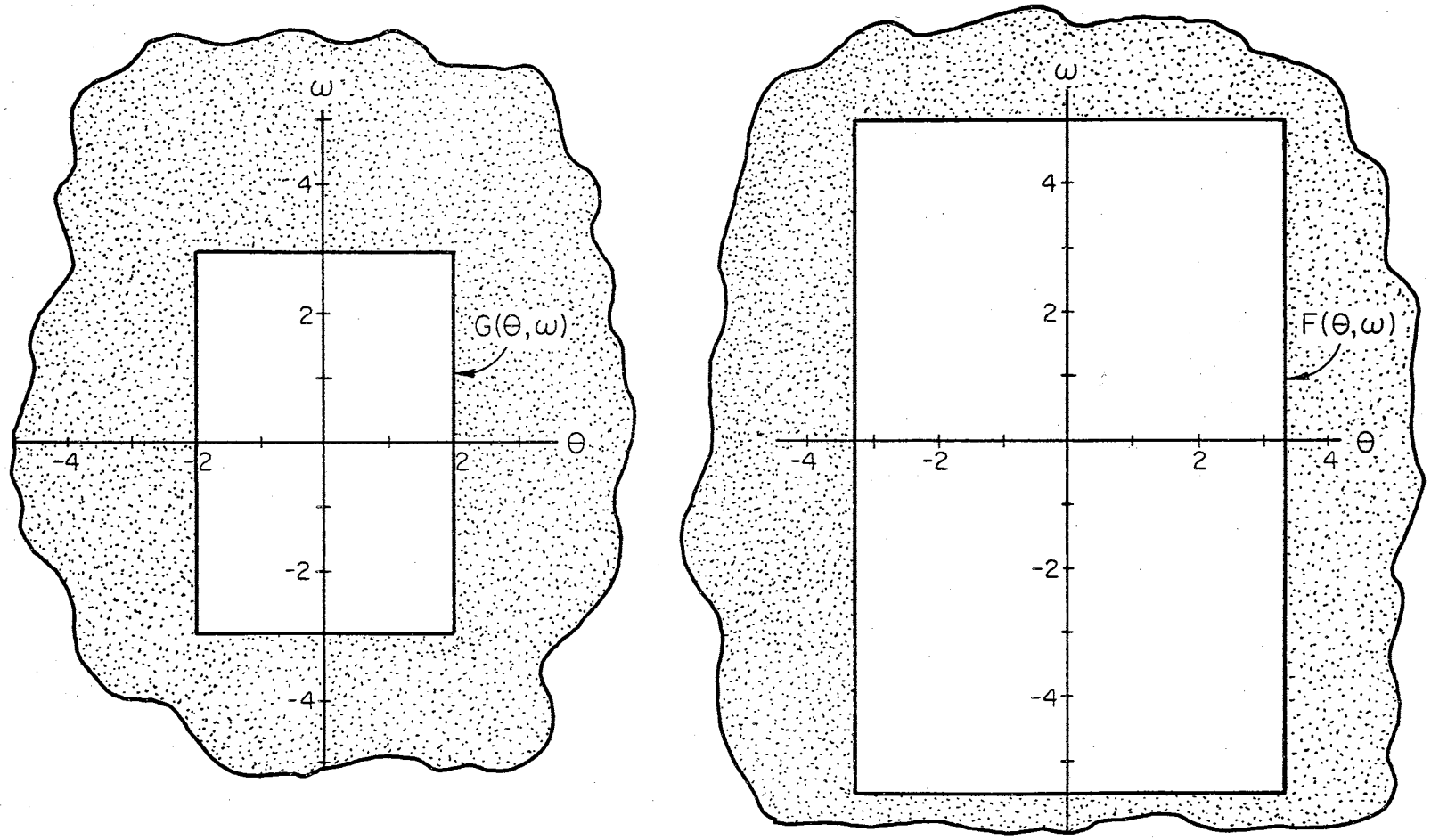

Figure 3. Example of Parent Image Function (Left) and K-Stretched Image Function (Right) for K=0.6

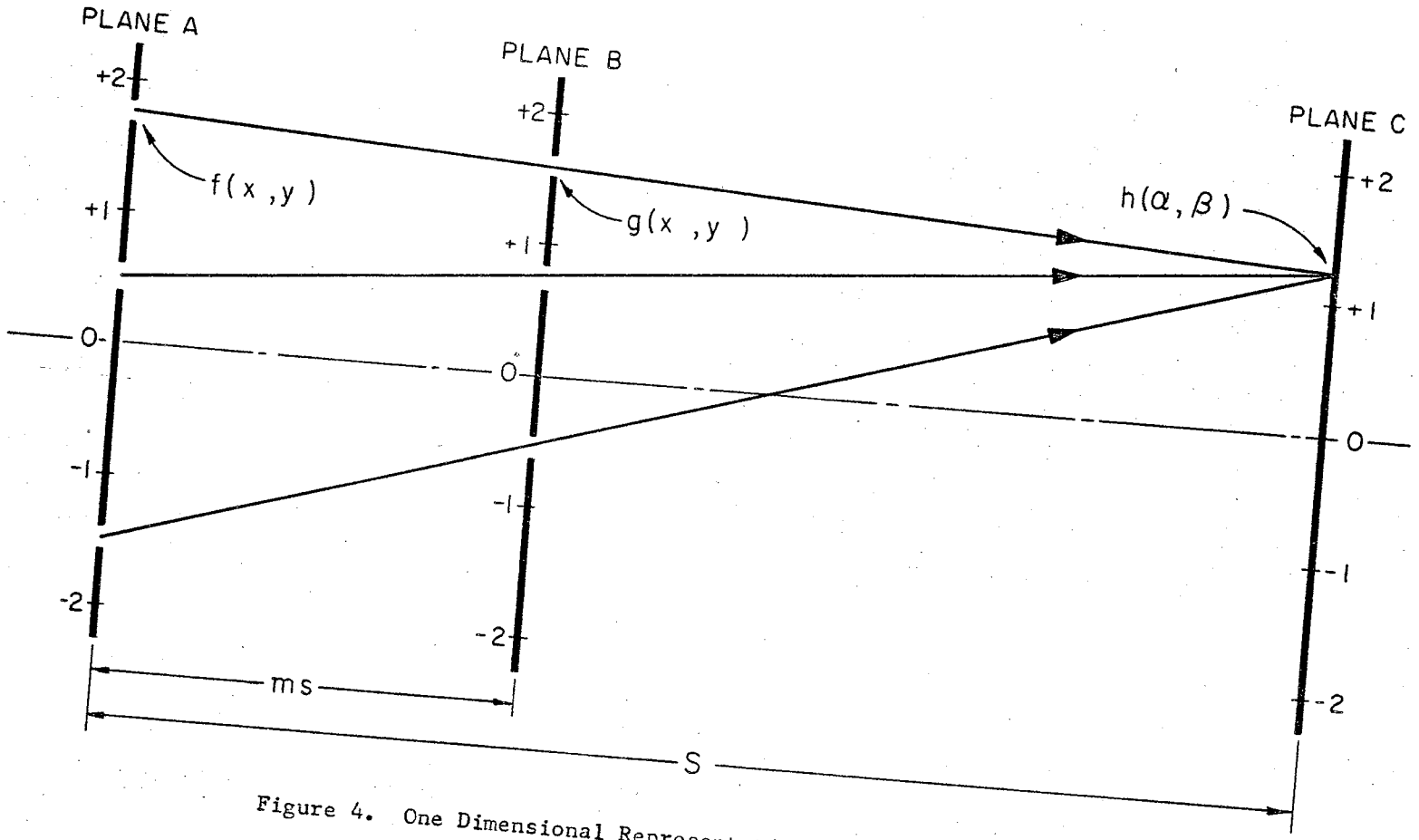

Figure 4. One Dimensional Representation of Light-Ray Geometry

straight line extending from the point (x_1, y_1) in plane A to the point (α, β) in plane C must intersect the point

$$x_2 = (1 - m)\, x_1 + m\alpha \quad , \quad y_2 = (1 - m)\, y_1 + m\beta$$

in plane B. Let I_0 represent the light intensity per unit area emanating from the planar diffused light source and impinging on the transparency in plane A. Further, let x_1' and x_1'', and y_1' and y_1'', respectively, be the maximum x-limits and y-limits of the A plane pattern represented by the transparency function $f(x_1, y_1)$. The detected light intensity function $h(\alpha, \beta)$ is then given by the equation

$$h(\alpha, \beta) = \int_{y_1'}^{y_1''} \int_{x_1'}^{x_1''} I_0 \cdot f(x_1, y_1) \cdot g\left[\{(1 - m)x_1 + m\alpha\}, \{(1 - m)y_1 + m\beta\}\right] dx_1 \cdot dy_1 \tag{2-4}$$

In view of this expression and the preceding definitions 1 and 2, the following theorem may be formulated with relation to the optical system represented by Figures 1 and 4.

THEOREM. If a dispersive light beam traverses a first plane containing a first transparency pattern $f(x, y)$, and then traverses a second plane containing a second transparency pattern $g(x, y)$ positioned at a distance ms from the first plane, and produces a two dimensional light intensity function $h(\alpha, \beta)$ by illuminating uniformly distributed light scattering elements in a third plane positioned at a distance $(1 - m)s$ from the second plane, and if $p(k\theta, k\omega)$ is defined as the k-stretched function whose parent image function is $p(\theta, \omega)$, then

$h(\alpha, \beta)$ is the m-stretched image function whose parent image function is the two dimensional cross correlation of the image function $f(x, y)$ against the $(1 - m)$-stretched image function whose parent image function is $g(x, y)$.

CHAPTER III

EXPERIMENTAL OPTICAL CORRELATION APPARATUS

Initial investigation of the two-dimensional correlation method involved the assembly of a system which implements the geometries described in Chapter II and Figure 1. An available projector, originally a combination slide and opaque projector (Bausch and Lomb, Type 41-23-81), was utilized for its light source and condensing lens system. In former use a pair of 4.3-inch-diameter lenses formed a conventional condensing lens system in which the light source is placed at one focal point of the first lens so that light leaving the first lens is essentially collimated into parallel rays; the second lens serves to converge the beam back to a point usually at the rear of the projection lens. In the modification the second lens of the condensing set was removed to allow the parallel rays to impinge normally upon the ground-glass diffuser. A mechanical carriage for the diffuser and first transparency was fabricated to fit the space normally occupied by the slide carrier. The carriage was constructed so that both the ground-glass diffuser and the first transparency could be inserted into the carriage separately.

The first transparency was positioned as close as possible to the ground-glass diffuser to make the plane of the diffused light source and the plane of the first pattern nearly coincident.

The second transparency was mounted in a second carriage comprised

by a modified sheet-film holder fastened to a mounting base located half-way (9.5 inches) between the first transparency and the observation plane.

The observation plane consisted of an 8-inch by 10-inch sheet of commercially available ground glass located 19 inches from the plane of the first transparency, mounted in a shadow box arranged to minimize the effects of stray light. The observation plane assembly is shown near the center of the picture in Figure 5.

A-Plane and B-Plane Image Transparency Design

The transparencies were made using commercially available 4x5-inch high contrast, orthochromatic, acetate-base film. The photographic process used was similar to that ordinarily used in producing film negatives, except for the exposure times required and the fact that the film could be developed in red safe-light. The latter fact was found helpful in that some compensation for exposure variation and developer temperature could be effected during development.

Images were typically made about 3 inches, and 1.5 inches, in height on the 4-inch dimension of the film for the A-plane, and B-plane respectively. The original images of interest in the preliminary studies were black figures on a white background, and were typically about one inch in height. A 3x and 1.5x magnification was thus required in the photography process for the A-plane and B-plane images, respectively. Although the initial exposure time for an image of one particular magnification was determined by experiment, exposure-time adjustments for various magnifications could be made by use of the following expres-

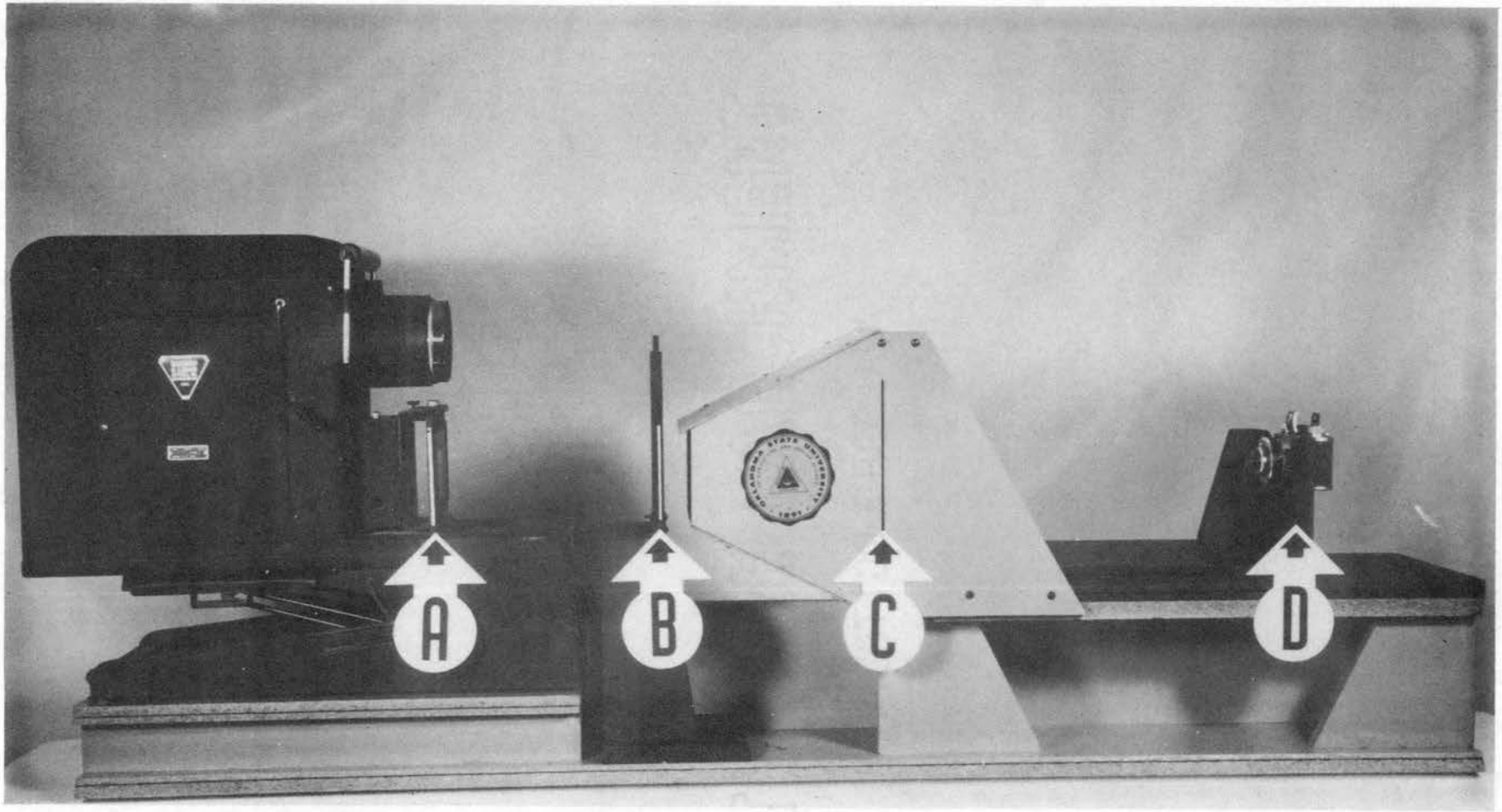

Figure 5. Experimental Optical Cross Correlator Showing (a) A-Plane Pattern Position, (b) B-Plane Pattern Position, (c) Observation Plane Position, and (d) 35 mm Camara For Recording Patterns

sion for image plane illumination

$$I = \frac{B}{4\ (1 + m)^2\ A^2} \tag{3-1}$$

where

I = image illumination in footcandles, metercandles, etc.

B = object luminance in footlamberts, meterlamberts, etc.

A = lens aperture (f/number)

m = magnification ratio

Since exposure is equal to the product of image illumination I and exposure time T, the exposure time for any magnification may be found by equating the expressions for exposure. That is

$$T_1 \cdot I_1 = T_2 \cdot I_2 \tag{3-2}$$

or

$$T_1 \cdot \frac{B}{4(1 + m_1)^2\ A_1^2} = T_2 \cdot \frac{B}{4(1 + m_2)^2\ A_2^2} \tag{3-3}$$

then given some satisfactory exposure time (T_1) and constant object luminance, the exposure time for any given magnification may be found as follows

$$T_2 = \frac{(1 + m_2)^2\ A_2^2}{(1 + m_1)^2\ A_1^2} \cdot T_1 \tag{3-4}$$

and further if the aperture is also held constant

$$T_2 = \frac{(1 + m_2)^2}{(1 + m_1)^2} \cdot T_1 \quad . \tag{3-5}$$

A press type camera (Folmer Graflex Corporation, Speed Graphic) with 127 mm, f/4.7 lens (Kodak, Ektar) and double extension bellows was

used for photographing the images for the A-plane and B-plane transparencies. The camera was equipped with both a focal plane shutter and the more common "between the lens" (Kodak, Supermatic Number 2) shutter but the focal plane shutter was not used in this case. An f/3.2, 4.5-inch-focal-length lens was mounted in an adapter ring (Kodak, Series VI) to augment the regular lens and achieve the image magnifications in the photography process mentioned previously.

Original images for preliminary experiments were drawn on "botany" paper with black drawing ink. Object illumination was provided by two ordinary 100-watt long-life incandescent bulbs mounted in common desk lamps, and located 8-to-10 inches from the image to be photographed. An improvised, track-mounted easel attached to a common base plate with the Graflex camera allowed convenient positioning of the image for proper magnification while minimizing problems of inadvertant movement of the image relative to the camera. The camera, easel, and base plate, plus one of the lamps, are shown in Figure 6.

For convenience, the same overall dimension was used for both the A-plane and B-plane transparencies. The maximum x-and-y extents of interest on the A and B transparencies were sized appropriately for the spacing between the A and B planes, and the B and C planes, i.e. for the B-plane located equidistant between planes A and C, the previously described coefficient m is 0.5 and the B-plane x-and-y extents of interest become one-half the respective x-and-y extents of interest in the A-plane. Figure 7 shows two of the transparencies used.

The basic exposure time determined by several trials was found to be 20 seconds for an aperture of f/22 and a 3x magnification of the

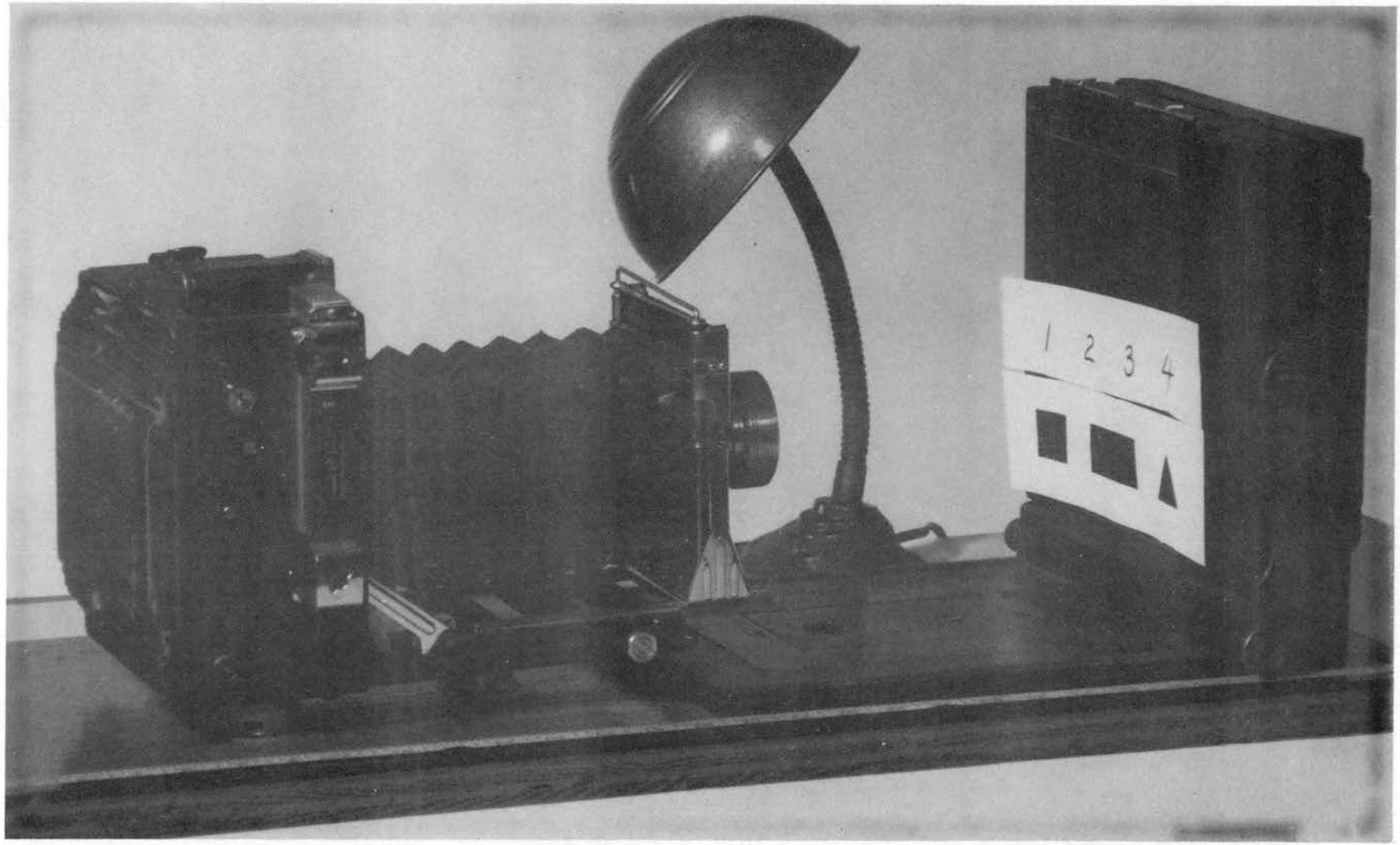

Figure 6. Graphic Camara and Track Mounted Easel Used for Photographing Patterns

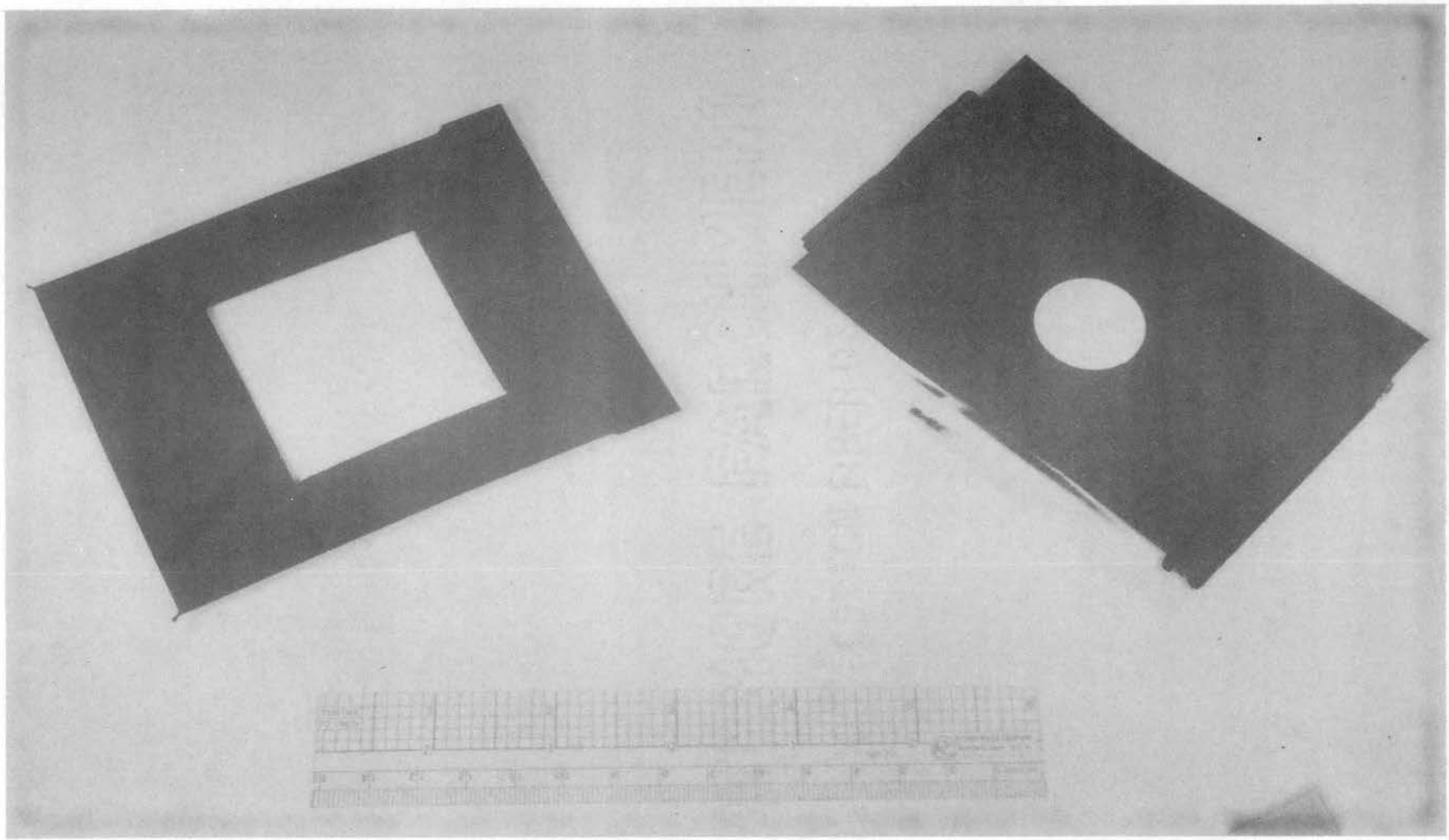

Figure 7. Actual Film Transparencies Used in Optical Correlation Experiments

object image. By use of Equation (3-5), exposure times of 8 seconds and 5 seconds were determined for the 1.5x and 1.0x magnifications, respectively. The determination of exposure times may be facilitated further by the use of a graph such as the one shown in Figure 8. In this case T_1 is the exposure time for a 1x magnification ($M_1 = 1$) and may be determined directly by experiment or from the graph, based on any other satisfactory exposure.

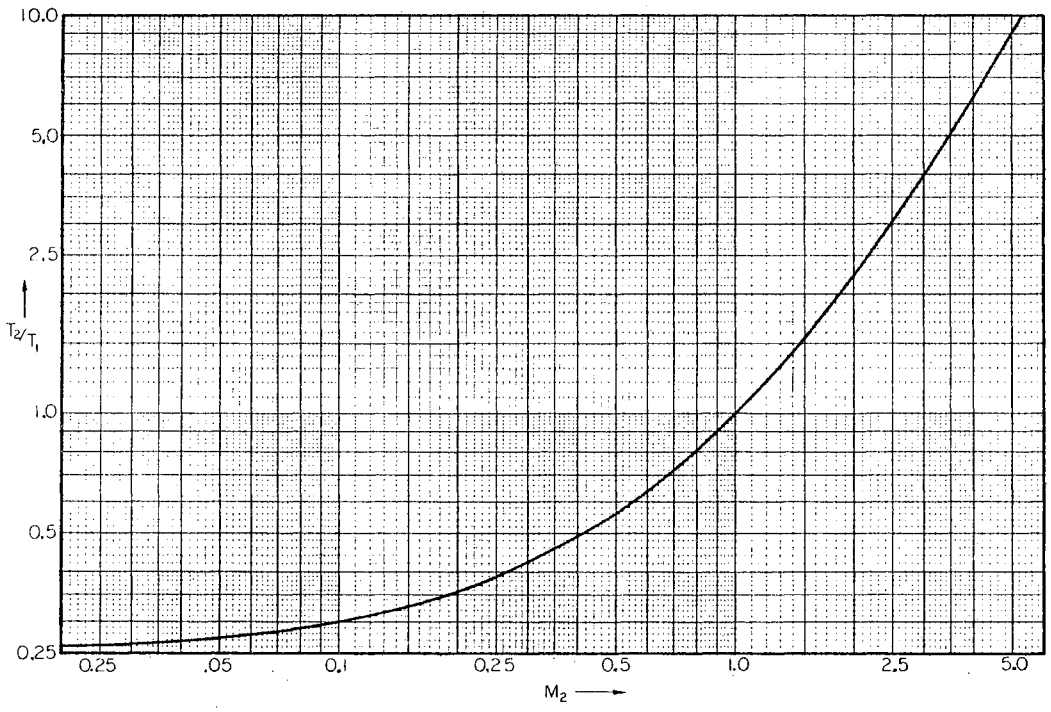

Figure 8. Graph for Determination of Relative Exposure Time

Recording Correlation Patterns

A 35 mm camera (Eastman Kodak Company, Kodak 35) was modified for use in recording the cross-correlation patterns produced on the observation plane. The front lens of the camera was extended to allow the observation plane to be photographed closely enough to fill the 35 mm-film negative. Forward movement of the lens to allow for the close-up photography required a different method of focusing since the original distance calibrations of the camera were no longer valid. A satisfactory focusing method was devised by placing a strip of material having light diffusing properties in the film guide of the camera. The image could then be focused in the same manner as with cameras equipped with a ground-glass plate.

The camera mounting was constructed so that the back could be removed from the camera for focusing and loading film without disturbing the position of the camera relative to the observation plane. A Graflex electrical shutter release solenoid was attached to the camera mounting plate to actuate the shutter release mechanism. The solenoid was energized by a Graflex battery package with its built-in push-button switch and connecting cord. The camera and mounting are shown at the extreme right in Figure 5.

Normal contrast film was used in recording the correlation patterns since the information sought is in the intensity level as well as the position of the illumination in the observation plane. Normal film negatives were made so that prints made from the film would indicate white for areas of illumination. If projection of the correlation patterns were desired, direct positive film could be used.

CHAPTER IV

EXPERIMENTAL VERIFICATION OF THEORETICAL PREDICTIONS

Some of the simpler geometric shapes provide a basis for comparing the experimental correlation results with those obtained mathematically. Results thus obtained through comparison of theory and experiment for simple patterns can then aid in the interpretation of more complex patterns. Results of the theoretical example to follow will be compared with corresponding experimental results obtained by use of the equipment described in the previous chapter.

Example

Figure 9 illustrates the relative displacements of two simple, nearly coplanar patterns, oriented for the determination of the conventional two-dimensional cross-correlation function. As previously noted, a transparency function value of zero represents complete opacity while a value of unity represents complete transparency. Since the transparency function over either of the pattern planes is either zero or unity, the unit step function

$$U(x) \equiv \begin{cases} 0, & x < 0 \\ 1, & x \geq 0 \end{cases}, \tag{4-1}$$

may be used conveniently in the computation of the cross correlation function of the two rectangles. In order to retain generality, it will

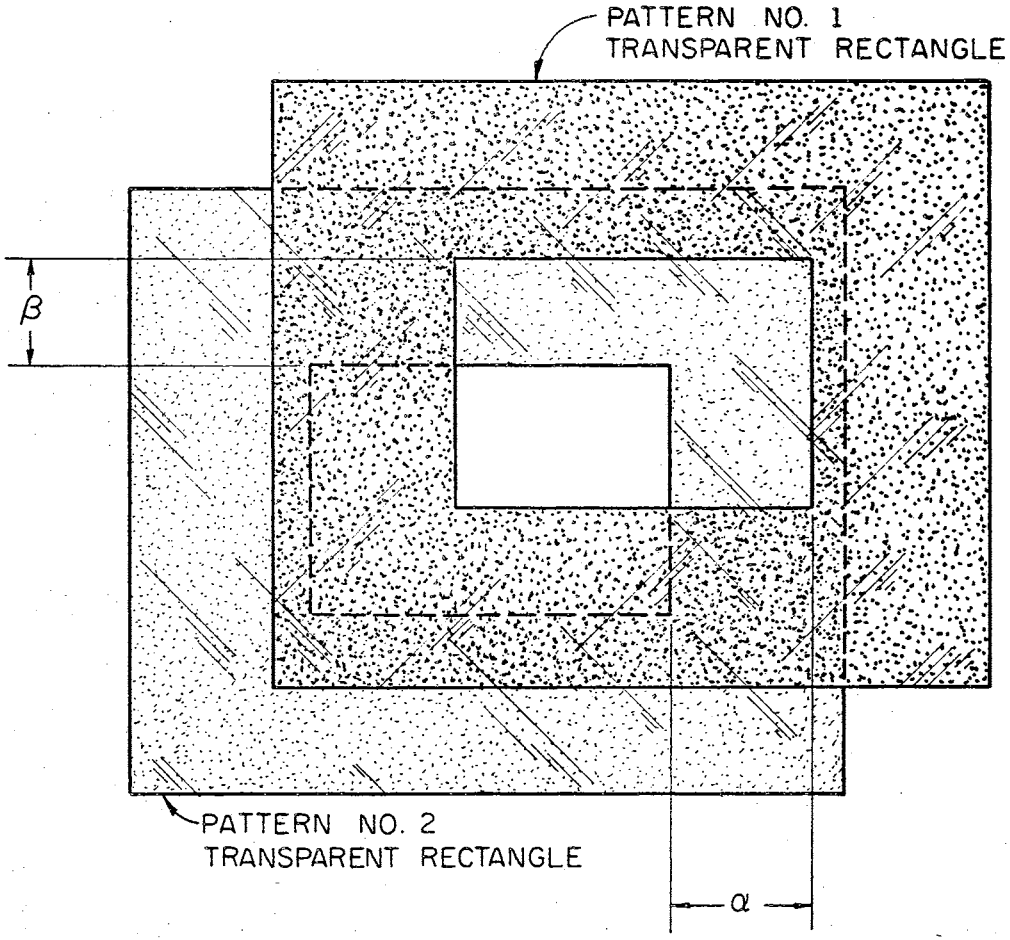

Figure 9. Illustration of Relative Displacement of Two Images to Obtain the Two-Dimensional Cross-Correlation Function $h(\alpha, \beta)$

be assumed in the initial computation that the first rectangle has dimensions a and b in the x and y coordinates, respectively, and the second rectangle has dimensions c and d in the x and y coordinates, respectively. It is also assumed that the rectangles are centered in their respective planes and that none of the dimensions exceed the extents of interest implied by the limits on the integrals. The cross-correlation function may then be expressed as

$$\rho(\alpha,\beta) = \int_{y_1'}^{y_1''} \int_{x_1'}^{x_1''} f(x,y)\, g(x+\alpha,\, y+\beta)\, dx\, dy \quad , \tag{4-2}$$

where

$$f(x,y) = \left[U(x+\tfrac{a}{2}) - U(x-\tfrac{a}{2})\right]\left[U(y+\tfrac{b}{2}) - U(y-\tfrac{b}{2})\right] \quad ,$$

and

$$g(x,y) = \left[U(x+\tfrac{c}{2}) - U(x-\tfrac{c}{2})\right]\left[U(y+\tfrac{d}{2}) - U(y-\tfrac{d}{2})\right] \quad .$$

The cross correlation function then becomes

$$\rho(\alpha,\beta) = \int_{y_1'}^{y_1''} \left[U(y+\tfrac{b}{2}) - U(y-\tfrac{b}{2})\right]\left[U(y+\tfrac{d}{2}+\beta) - U(y-\tfrac{d}{2}-\beta)\right] \cdot \int_{x_1'}^{x_1''} \left[U(x+\tfrac{a}{2}) - U(x-\tfrac{a}{2})\right]\left[U(x+\alpha+\tfrac{c}{2}) - U(x+\alpha-\tfrac{c}{2})\right] dx\, dy \quad . \tag{4-3}$$

If the inside integral above is identified as $\rho_1(\alpha)$, then

$$\rho_1(\alpha) = \int_{x_1'}^{x_1''} U(x+\tfrac{a}{2})\, U(x+\alpha+\tfrac{c}{2})dx - \int_{x_1'}^{x_1''} U(x+\tfrac{a}{2})\, U(x+\alpha-\tfrac{c}{2})dx - \int_{x_1'}^{x_1''} U(x-\tfrac{a}{2})\, U(x+\alpha+\tfrac{c}{2})dx + \int_{x_1'}^{x_1''} U(x-\tfrac{a}{2})\, U(x+\alpha-\tfrac{c}{2})dx \quad , \tag{4-4}$$

which further simplifies to

$$\rho_1(\alpha) = \int_{-\frac{a}{2}}^{\frac{a}{2}} U(x + \alpha + \tfrac{c}{2})dx - \int_{-\frac{a}{2}}^{\frac{a}{2}} U(x + \alpha - \tfrac{c}{2})dx \quad . \qquad (4\text{-}5)$$

The resulting value of the function $\rho_1(\alpha)$ depends on the relative magnitudes of the x dimensions of the f(x, y) and g(x, y) patterns. If $c < a$, then

$$\rho_1(\alpha) = \begin{cases} 0 , & \alpha \leq -(\frac{a+c}{2}) \\ \alpha + \frac{c+a}{2}, & -(\frac{a+c}{2}) \leq \alpha \leq \frac{c-a}{2} \\ c , & \frac{c-a}{2} \leq \alpha \leq \frac{a-c}{2} \\ \frac{c+a}{2} - \alpha, & \frac{a-c}{2} \leq \alpha \leq \frac{a+c}{2} \\ 0 , & \alpha \geq \frac{2+c}{2} \end{cases} \qquad (4\text{-}6)$$

If $c > a$, then

$$\rho_1(\alpha) = \begin{cases} 0 , & \alpha \leq -(\frac{a+c}{2}) \\ \alpha + \frac{c+a}{2}, & -(\frac{a+c}{2}) \leq \alpha \leq \frac{a-c}{2} \\ a , & \frac{a-c}{2} \leq \alpha \leq \frac{c-a}{2} \\ \frac{c+a}{2} - \alpha, & \frac{c-a}{2} \leq \alpha \leq \frac{c+a}{2} \\ 0 , & \alpha \geq \frac{c+a}{2} \end{cases} \qquad (4\text{-}7)$$

Finally, if $c = a$, which implies $(a + c)/2 = a = c$ and $a - c = c - a = 0$, then

$$\rho_1(\alpha) = \begin{cases} 0 , & \alpha \leq -a \\ \alpha + a , & -a \leq \alpha \leq 0 \\ a - \alpha , & 0 \leq \alpha \leq a \\ 0 , & \alpha \geq a \end{cases} . \tag{4-8}$$

Substitution of $\rho_1(\alpha)$ thus determined into Equation (4-3) yields

$$\rho(\alpha, \beta) = \rho_1(\alpha) \int_{-\frac{b}{2}}^{\frac{b}{2}} U(y + \frac{d}{2} + \beta)dy - \int_{-\frac{b}{2}}^{\frac{b}{2}} U(y - \frac{d}{2} + \beta)\, dy. \tag{4-9}$$

If the quantity in the brackets in Equation (4-9) is identified as $\rho_2(\beta)$, then

$$\rho(\alpha, \beta) = \rho_1(\alpha) \cdot \rho_2(\beta) . \tag{4-10}$$

The value of the function $\rho_2(\beta)$ depends on the relative magnitudes of the y dimensions of the $f(x, y)$ and $g(x, y)$ patterns. If $d < b$, then

$$\rho_2(\beta) = \begin{cases} 0 , & \beta \leq -\frac{(b + d)}{2} \\ \beta + \frac{b + d}{2}, & -\frac{(b + d)}{2} \leq \beta \leq \frac{d - b}{2} \\ d , & \frac{d - b}{2} \leq \beta \leq \frac{b - d}{2} \\ \frac{b + d}{2} - \beta, & \frac{b - d}{2} \leq \beta \leq \frac{b + d}{2} \\ 0 , & \beta \geq \frac{b + d}{2} \end{cases} . \tag{4-11}$$

If $d > b$, then

$$\rho_2(\beta) = \begin{cases} 0 , & \beta \leq -\frac{(b+d)}{2} \\ \beta + \frac{b+d}{2}, & -\frac{(b+d)}{2} \leq \beta \leq \frac{(b-d)}{2} \\ b , & \frac{(b-d)}{2} \leq \beta \leq \frac{(d-b)}{2} \\ \frac{b+d}{2} - \beta, & \frac{(d-b)}{2} \leq \beta \leq \frac{d+b}{2} \\ 0 , & \beta \geq \frac{b+d}{2} \end{cases} ; \tag{4-12}$$

finally, if $d = b$, then

$$\rho_2(\beta) = \begin{cases} 0 , & \beta \leq b \\ \beta + b , & -b \leq \beta \leq 0 \\ b - \beta , & 0 \leq \beta \leq b \\ 0 , & \beta \geq b \end{cases} \tag{4-13}$$

The functions $\rho_1(\alpha)$ and $\rho_2(\beta)$ can be defined more briefly in terms of absolute value symbols. Equations (4-6), (4-7) and (4-8) may thus be expressed as

$$\rho_1(\alpha) = \begin{cases} 0 , & |\alpha| \geq \left|\frac{a+c}{2}\right| \\ \frac{a+c}{2} - |\alpha|, & \left|\frac{a-c}{2}\right| \leq |\alpha| \leq \left|\frac{a+c}{2}\right| \\ c , & |\alpha| \leq \left|\frac{a-c}{2}\right| , \ c < a \\ a , & |\alpha| \leq \left|\frac{a-c}{2}\right| , \ a < c \end{cases} . \tag{4-14}$$

Similarly, Equations (4-11), (4-12) and (4-13) may be combined to obtain

$$\rho_2(\beta) = \begin{cases} 0 , & |\beta| \geq \left|\frac{b+d}{2}\right| \\ \frac{b+d}{2} - |\beta| , & \left|\frac{b-d}{2}\right| \leq |\beta| \leq \left|\frac{b+d}{2}\right| \\ d , & |\beta| \leq \left|\frac{b-d}{2}\right| , \; d < b \\ b , & |\beta| \leq \left|\frac{b-d}{2}\right| , \; b < d \; . \end{cases} \tag{4-15}$$

If the first pattern function f(x, y) is a square with side lengths equal to 2 units and the second pattern function g(x, y) is a rectangle with x-dimension equal to 4 units and y-dimension equal to 2 units, then

$$f(x, y) = [U(x + 1) - U(x - 1)]\,[U(y + 1) - U(y - 1)]$$

and

$$g(x, y) = [U(x + 2) - U(x - 2)]\,[U(y + 1) - U(y - 1)] \; .$$

In this case above the constituent parts of the cross-correlation function may be expressed as

$$\rho_1(\alpha) = \begin{cases} 0 & |\alpha| \geq 3 \\ 3 - |\alpha| , & 1 \leq |\alpha| \leq 3 \\ 2 , & |\alpha| \leq 1 \end{cases} \tag{4-16}$$

and

$$\rho_2(\beta) = \begin{cases} 0 , & |\beta| \geq 2 \\ 2 - |\beta| , & 2 \geq |\beta| \; . \end{cases} \tag{4-17}$$

A three-dimensional representation of the product $\rho(\alpha,\beta) = \rho_1(\alpha) \cdot \rho_2(\beta)$ of the above functions is illustrated in Figure 10. The top view in Figure 10 shows several equal value contours of $\rho(\alpha,\beta)$ while the perspective view shows the general shape. In interpreting this theoretically obtained function $\rho(\alpha,\beta)$ in terms of an equivalent light intensity function $h(\alpha,\beta)$, it will be expected that the illumination of points in the α, β plane will be more intense at points where $\rho(\alpha,\beta)$ has the largest value.

A photograph of the experimental result corresponding to the theoretical patterns illustrated in Figure 10 is shown in Figure 11. Agreement between the experimental result and the theoretical prediction is seen in the photographic presence of the intensified straight lines which correspond to the "high ridges" seen in the perspective projection of the theoretically predicted light intensity pattern.

In obtaining the photographed experimental result shown in Figure 11, it was found necessary to compensate for the imperfection of the ground-glass light scattering slab used to realize experimentally the planar diffused light source identified in Figure 1. Preliminary experiments with the apparatus illustrated in Figure 5 showed that the light beam impinging on the light scattering slab was not scattered uniformly in all directions, but rather was more strongly scattered in the forward direction than in other directions. This generally caused the center of the photographed detection plane to be too brightly illuminated. Compensation for this imperfection was achieved by insertion of additional light diffusing material in the center of the light scattering slab. Alternatively, compensation for the diffuser imperfection could be achieved by the deliberate misalignment of the impinging light beam axis.

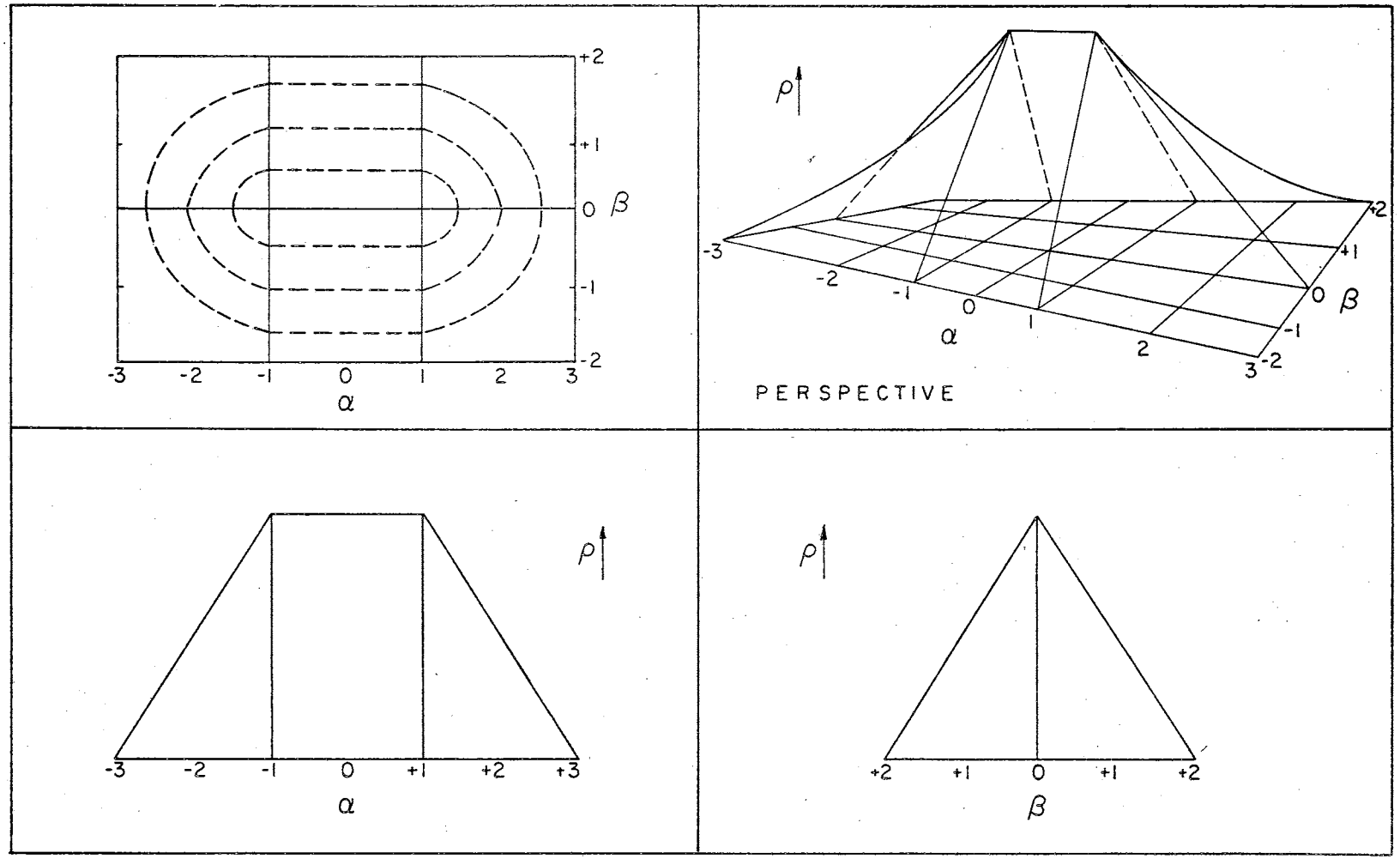

Figure 10. Three-Dimensional Representation of the Two-Dimensional Cross-Correlation Function for Two Rectangular Patterns for Which a = 2, b = 2, c = 4, and d = 2

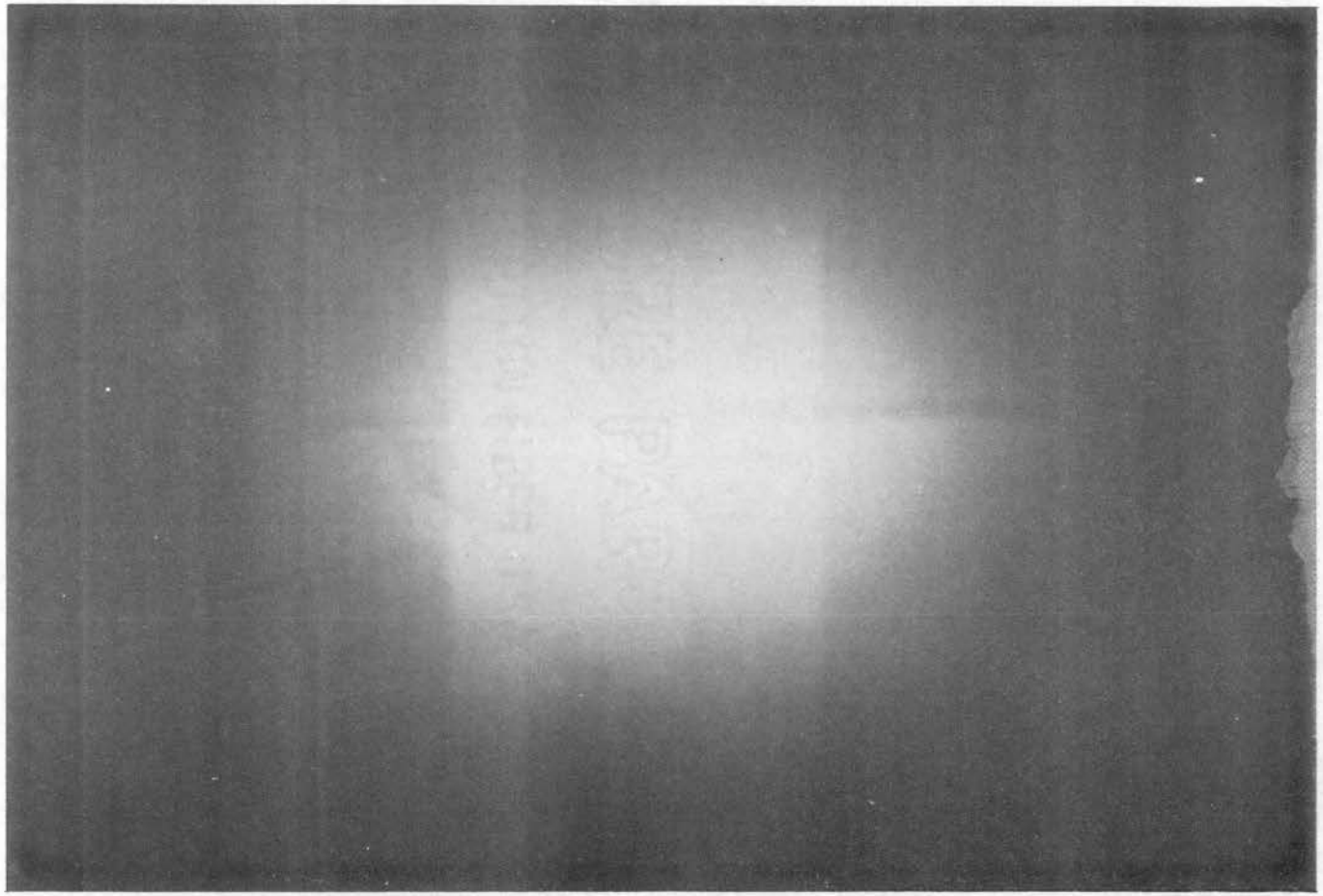

Figure 11. Actual Light Intensity Function Recorded From Optical Cross-Correlator For Two Rectangular Transparencies, For Which a = b = d = 4 and c = 4

However, this was found to introduce undesirable distortion of the image geometry.

As a further comparison of the theoretical predictions with experimental results, the special case in which the two patterns were identical squares was examined. In this special case Equations (4-10), (4-14) and (4-15) give

$$\rho(\alpha, \beta) = \begin{cases} \left[a - |\alpha|\right] \cdot \left[a - |\beta|\right], & |\alpha| \leq a \\ & |\beta| \leq a \\ 0 & \text{elsewhere} \end{cases}$$

in which a = b = c = d = 2 units. This relationship is illustrated graphically in Figure 12. A photograph of the corresponding experimental result is shown in Figure 13.

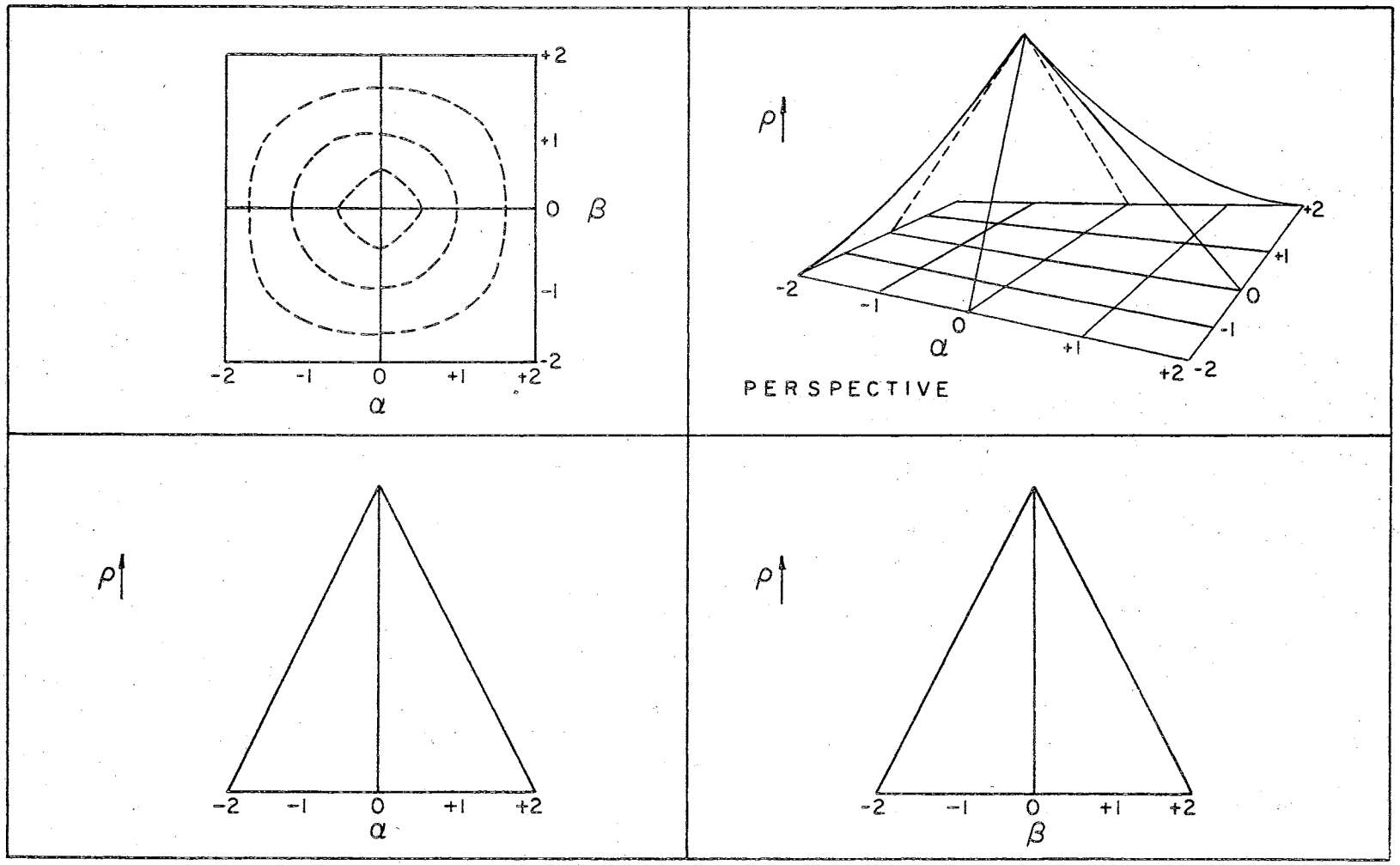

Figure 12. Three-Dimensional Representation of the Two-Dimensional Cross-Correlation Function for Two Square Patterns for Which a = b = c = d = 2

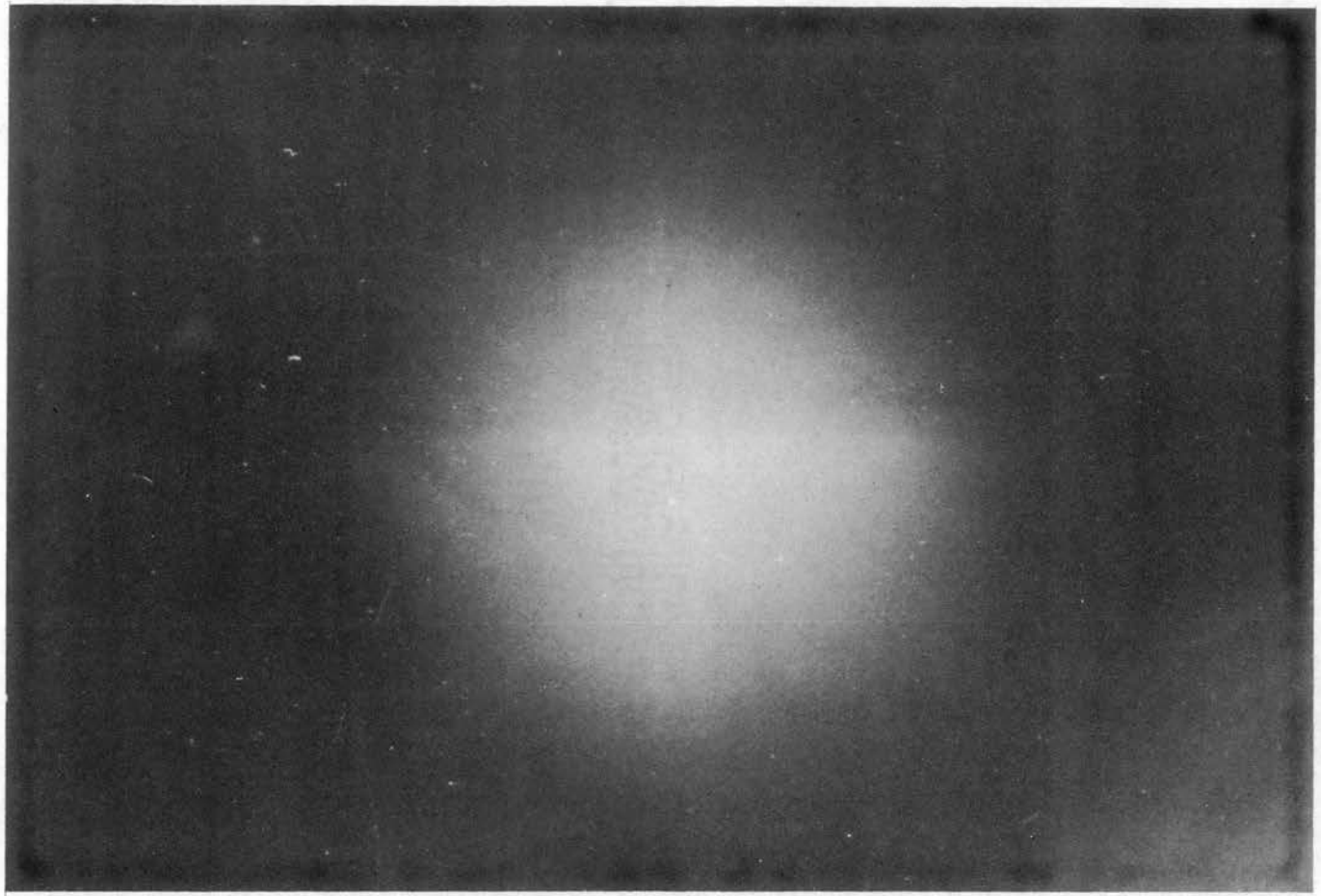

Figure 13. Actual Light Intensity Function Recorded From Optical Cross-Correlator For Two Square Transparencies, For Which $a = b = c = d = 2$

CHAPTER V

CALCULATED AND MEASURED PATTERNS

Repeated patterns in one or both planes of the optical cross correlator provide a basis for investigating the spatial-frequency (repetition per unit distance) characteristics of the resulting cross-correlation functions. These functions also provide at least some insight into possible applications of the optical cross-correlation technique.

Stripes whose lengths were several times their respective widths were chosen for the repeated pattern experiments and the mathematical analysis was simplified by carrying out calculations in one dimension only. To further expedite the gathering of data for the following experiments, the C-plane ground-glass diffuser was replaced with an easel for photographic paper and the experimental correlation functions were recorded directly on the photographic paper. The images from these recorded patterns are therefore negative functions such that a C-plane value of zero (zero or low light intensity) corresponds to white and a value of increasing positive value (increasing light intensity) corresponds to increasing densities of gray or black.

The approach used in the calculation of the predicted functions was to choose the simplest integrable function that would adequately describe the A-plane and B-plane functions and still give interpretable functions for comparison to the experimental results.

The B-plane pattern in all of the following cases was a repeated

pattern of vertical stripes with transparency and opacity widths equal, as would be approximated by a sine-squared transparency function. The entire available space in the x-dimension was used for the repeated stripe pattern and in the particular case of the following experiments this allowed the use of twelve stripes.

Experiment One

Let the first pattern be one stripe of width w. Necessary restrictions on w evolve from later calculations. The second pattern is the series of stripes mentioned earlier. The single stripe is described by a unit step function while the series of stripes is described by a sine-squared function. The particulars of the experiment are depicted in Figure 14.

In one dimension the cross-correlation function may be written

$$\rho(\alpha) = \int_{-\infty}^{\infty} f(x)\ g(x + \alpha)dx \tag{5-1}$$

where

$$f(x) = \left[U(x + \tfrac{w}{2}) - U(x - \tfrac{w}{2})\right]$$

then

$$\rho(\alpha) = \int_{-\infty}^{\infty} \left[U(x + \tfrac{w}{2}) - U(x - \tfrac{w}{2})\right] \cdot \sin^2 2\pi\left(\frac{x + \alpha}{L}\right)\ dx \tag{5-2}$$

or

$$\rho(\alpha) = \int_{-\frac{w}{2}}^{\frac{w}{2}} \sin^2 2\pi\left(\frac{x + \alpha}{L}\right)\ dx = \frac{1}{2}\int_{-\frac{w}{2}}^{\frac{w}{2}} \left[1 - \cos\frac{4\pi}{L}\ (x + \alpha)\right]dx \tag{5-3}$$

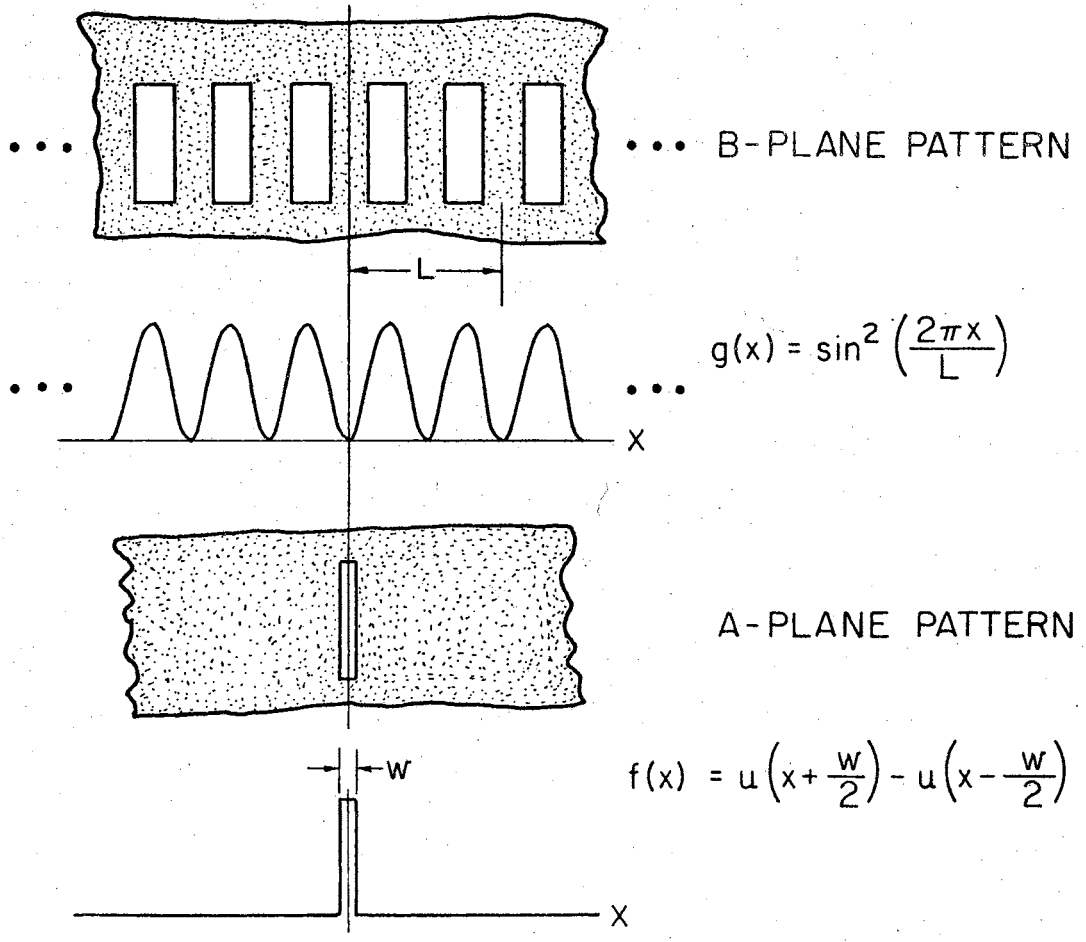

Figure 14. Images and Functions Used in Experiment One

Integration of Equation (5-3) with respect to x yields

$$\rho(\alpha) = \frac{1}{2}\left[x - \frac{L}{4\pi}\sin\frac{4\pi}{L}(x+\alpha)\right]_{-\frac{w}{2}}^{\frac{w}{2}} \qquad (5\text{-}4)$$

Evaluation of the limits and collection of terms yields

$$\rho(\alpha) = \frac{1}{2}\left\{w - \frac{L}{4\pi}\left[\sin\frac{4\pi}{L}\left(\alpha+\frac{w}{2}\right) - \sin\frac{4\pi}{L}\left(\alpha-\frac{w}{2}\right)\right]\right\} \qquad (5\text{-}4a)$$

which may be further simplified to give

$$\rho(\alpha) = \frac{1}{2}\left[w - \frac{L}{2\pi}\cos\left(\frac{4\pi}{L}\cdot\alpha\right)\sin\left(\frac{4\pi}{L}\cdot\frac{w}{2}\right)\right] \quad . \qquad (5\text{-}5)$$

For small values of (2 w/L), the function

$$\sin\left(\frac{2\pi\, w}{L}\right) \simeq \frac{2\pi\, w}{L}$$

and therefore Equation (5-5) may be approximated by

$$\rho(\alpha) \simeq \frac{L}{2\pi}\left(\sin\frac{2\pi\, w}{L}\right)\left[1 - \cos\left(\frac{4\pi}{L}\cdot\alpha\right)\right] \qquad (5\text{-}6)$$

or

$$\rho(\alpha) \simeq \frac{L}{2\pi}\left(\frac{2\pi\, w}{L}\right)\left[1 - \cos\left(\frac{4\pi}{L}\cdot\alpha\right)\right] \qquad (5\text{-}6a)$$

and by application of the trigonometric identity used previously

$$\rho(\alpha) \simeq w\left[\sin^2\left(2\pi\,\frac{\alpha}{L}\right)\right] \quad . \qquad (5\text{-}7)$$

The equation above shows that the resultant magnitude of the correlation function should vary directly as the width of the single A-plane stripe, and should retain the same spatial frequency and shape as the B-plane function. A record of the experimental result is shown in Figure 15. It is seen that the experimental result corresponds in general with the theoretical prediction of Equation (5-7). The "pincushion" appearance

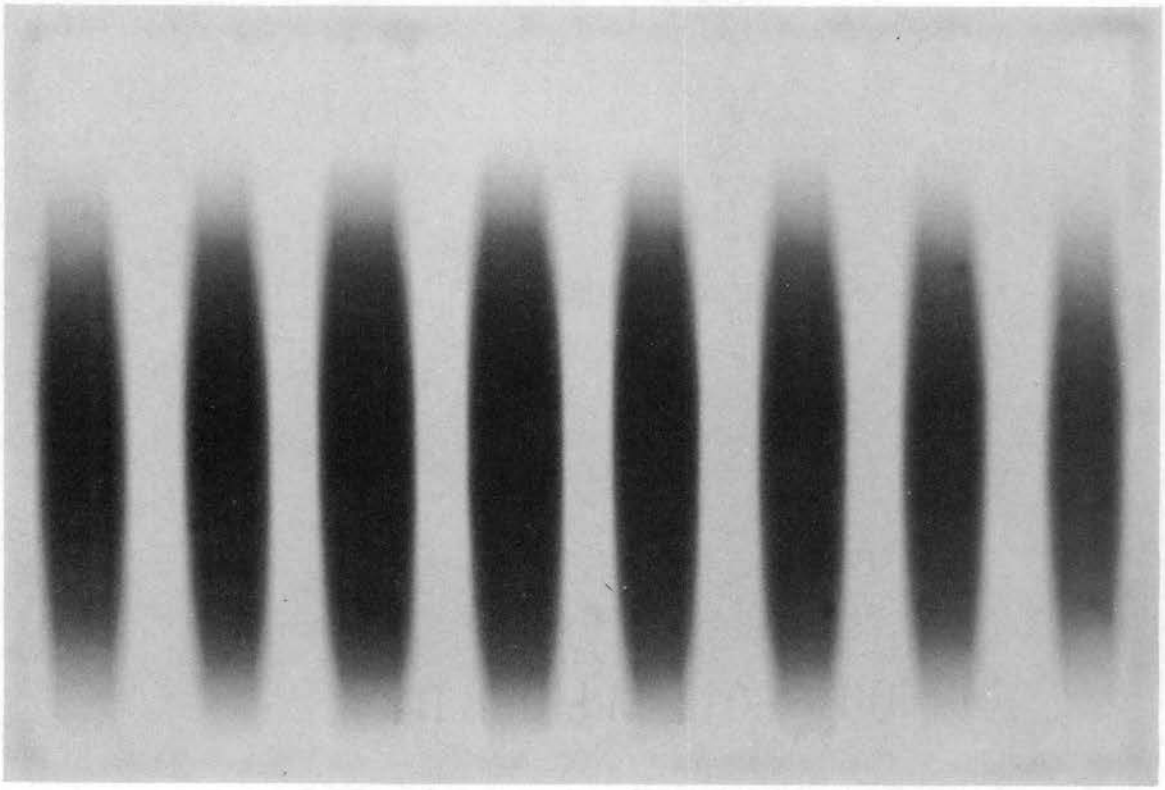

Figure 15. Cross-Correlation Results of Experiment One

of the image in Figure 15 is due, at least in part, to the reflection of light passing through the photographic paper by the focusing surface of the easel. When the paper is exposed some of the light in the higher intensity areas penetrates the paper, is diffused by the paper, reflects off the easel, is diffused again by the paper and adds undesired exposure to areas adjacent to points of desired exposure.

Experiment Two

The second experiment is depicted in Figure 16 and consists of the B-plane pattern described previously and an A-plane pattern comprising

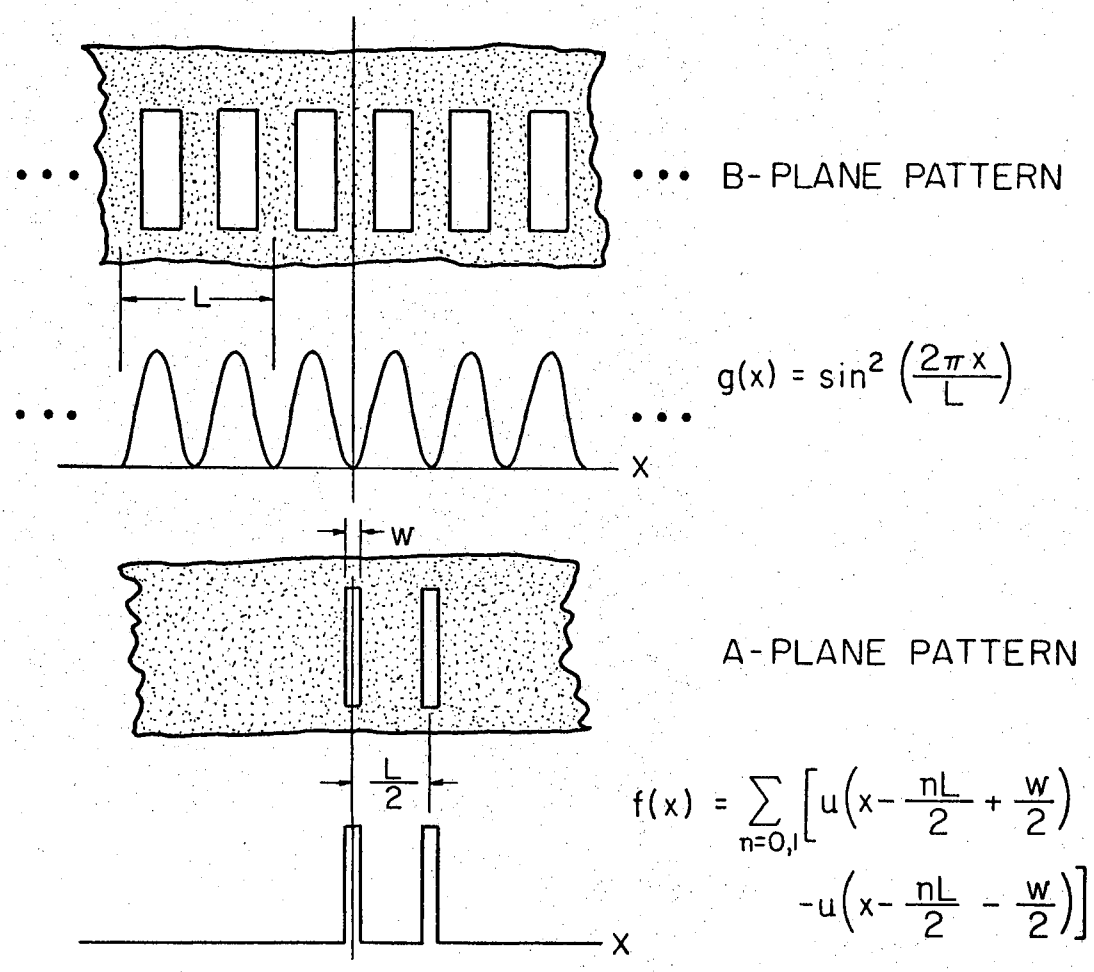

Figure 16. Images and Functions Used in Experiment Two

two stripes with center-to-center spacing of L/2 units. The cross-correlation function is again

$$\rho(\alpha) = \int_{-\infty}^{\infty} f(x)\ g(x + \alpha)\ dx \quad .$$

Use of the functions pertinent to this second experiment gives

$$\rho(\alpha) = \int_{-\infty}^{\infty} \left[u(x + \tfrac{w}{2}) - u(x - \tfrac{w}{2}) + u(x + \tfrac{w}{2} - \tfrac{L}{2}) - u(x - \tfrac{w}{2} - \tfrac{L}{2})\right] \cdot \sin^2\left[\frac{2\pi(x + \alpha)}{L}\right] dx \qquad (5\text{-}8)$$

and

$$\rho(\alpha) = \int_{-\frac{w}{2}}^{\frac{w}{2}} \sin^2 \frac{2\pi}{L}(x+\alpha)\,dx + \int_{\frac{L-w}{2}}^{\frac{L+w}{2}} \sin^2 \frac{2\pi}{L}(x+\alpha)\,dx \,. \qquad (5\text{-}9)$$

This expression reduces to

$$\rho(\alpha) = \tfrac{1}{2}\left[x - \frac{L}{4\pi}\sin\frac{4\pi}{L}(x+\alpha)\right]_{-\frac{w}{2}}^{\frac{w}{2}} + \tfrac{1}{2}\left[x - \frac{L}{4\pi}\sin\frac{4\pi}{L}(x+\alpha)\right]_{\frac{L-w}{2}}^{\frac{L+w}{2}} \qquad (5\text{-}10)$$

$$= \tfrac{1}{2}\left[\frac{w}{2} - \frac{L}{4\pi}\sin\frac{4\pi}{L}(\alpha+\tfrac{w}{2}) + \frac{w}{2} + \frac{L}{4\pi}\sin\frac{4\pi}{L}(\alpha-\tfrac{w}{2})\right]$$

$$+ \tfrac{1}{2}\left[\frac{L+w}{2} - \frac{L}{4\pi}\sin\frac{4\pi}{L}(\alpha+\frac{L+w}{2}) - (\frac{L-w}{2}) + \frac{L}{4\pi}\sin(\alpha+\frac{L-w}{2})\right] . \qquad (5\text{-}11)$$

Equation (5-11) may be simplified by use of trigonometric identities as follows

$$\rho(\alpha) = \tfrac{1}{2}\left\{w - \frac{L}{4\pi}\left[\sin\frac{4\pi}{L}(\alpha+\tfrac{w}{2}) + \sin\frac{4\pi}{L}(\alpha-\tfrac{w}{2})\right]\right\} \qquad (5\text{-}12)$$

$$+ \tfrac{1}{2}\left\{w - \frac{L}{4\pi}\left[\sin\frac{4\pi}{L}(\alpha+\tfrac{w}{2})\cos\frac{4\pi}{L}(\tfrac{L}{2}) + \cos\frac{4\pi}{L}(\alpha+\tfrac{w}{2})\sin\frac{4\pi}{L}(\tfrac{L}{2})\right.\right.$$

$$\left.\left. - \sin\frac{4\pi}{L}(\alpha-\tfrac{w}{2})\cos\frac{4\pi}{L}(\tfrac{L}{2}) - \cos\frac{4\pi}{L}(\alpha-\tfrac{w}{2})\sin\frac{4\pi}{L}(\tfrac{L}{2})\right]\right\}$$

yielding

$$\rho(\alpha) = w - \frac{L}{4\pi}\left[\sin\frac{4\pi}{L}(\alpha+\tfrac{w}{2}) - \sin\frac{4\pi}{L}(\alpha-\tfrac{w}{2})\right] , \qquad (5\text{-}13)$$

or

$$\rho(\alpha) = w - \frac{L}{4\pi}\cos(\frac{4\pi\alpha}{L}) \cdot \sin(\frac{4\pi}{L}\ \frac{w}{2}) \qquad (5\text{-}14)$$

It may be noted at this point, before simplification, that the predicted cross-correlation function $\rho(\alpha)$ for this second experiment is just twice that predicted in Equation (5-5) for the first experiment. Equation (5-14) may be simplified in the same manner as was Equation (5-5) to yield

$$\rho(\alpha) \approx 2w \left[\sin^2 \left(2\pi \frac{\alpha}{L}\right)\right] \quad . \tag{5-15}$$

The corresponding experimental results are shown in Figure 17. Although the results appear almost identical, it should be noted that the exposure time for the record of Figure 17 was one-half that for the record of Figure 15. It may thus be noted that the similarity of Equations (5-7) and (5-9), except for scale factor, is evident in the experimental results as well.

Experiment Three

Figure 18 depicts the third experiment in which the A-plane pattern comprised three stripes with center-to-center spacing between adjacent stripes of L/2 units. The calculation of the cross-correlation function yields

$$\rho(\alpha) = \frac{3}{2}\left[w - \frac{L}{4\pi} \cos \left(\frac{4\pi}{L} \alpha\right) \cdot \sin \left(\frac{4\pi}{L} \frac{w}{2}\right)\right] \quad . \tag{5-16}$$

This expression shows that for three stripes, the predicted function should be just three times that of Equation (5-5). Equation (5-16) may be simplified in a manner similar to Equations (5-5) and (5-14) to yield

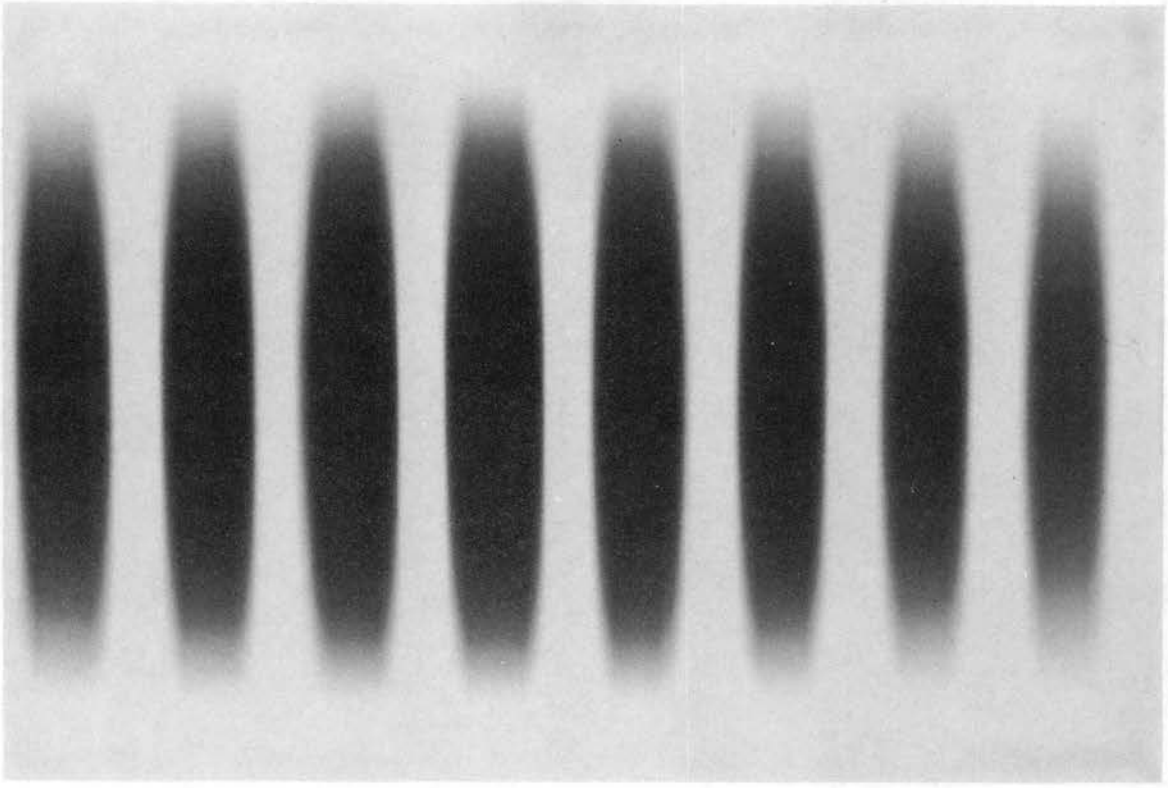

Figure 17. Cross-Correlation Results of Experiment Two

$$\rho(\alpha) \approx 3w \left[\sin^2 \left(2\pi \frac{\alpha}{L} \right) \right] . \qquad (5\text{-}17)$$

The corresponding experimental results are shown in Figure 19. Again intensity compensation was made by adjusting the exposure time. The record of Figure 19 was exposed for one-third the time that the record of Figure 15 was exposed.

In each of the previous experiments the center-to-center spacing of the A-plane stripes was equal to the center-to-center spacing of the B-plane stripes. Non-integral relationships between the spacings of

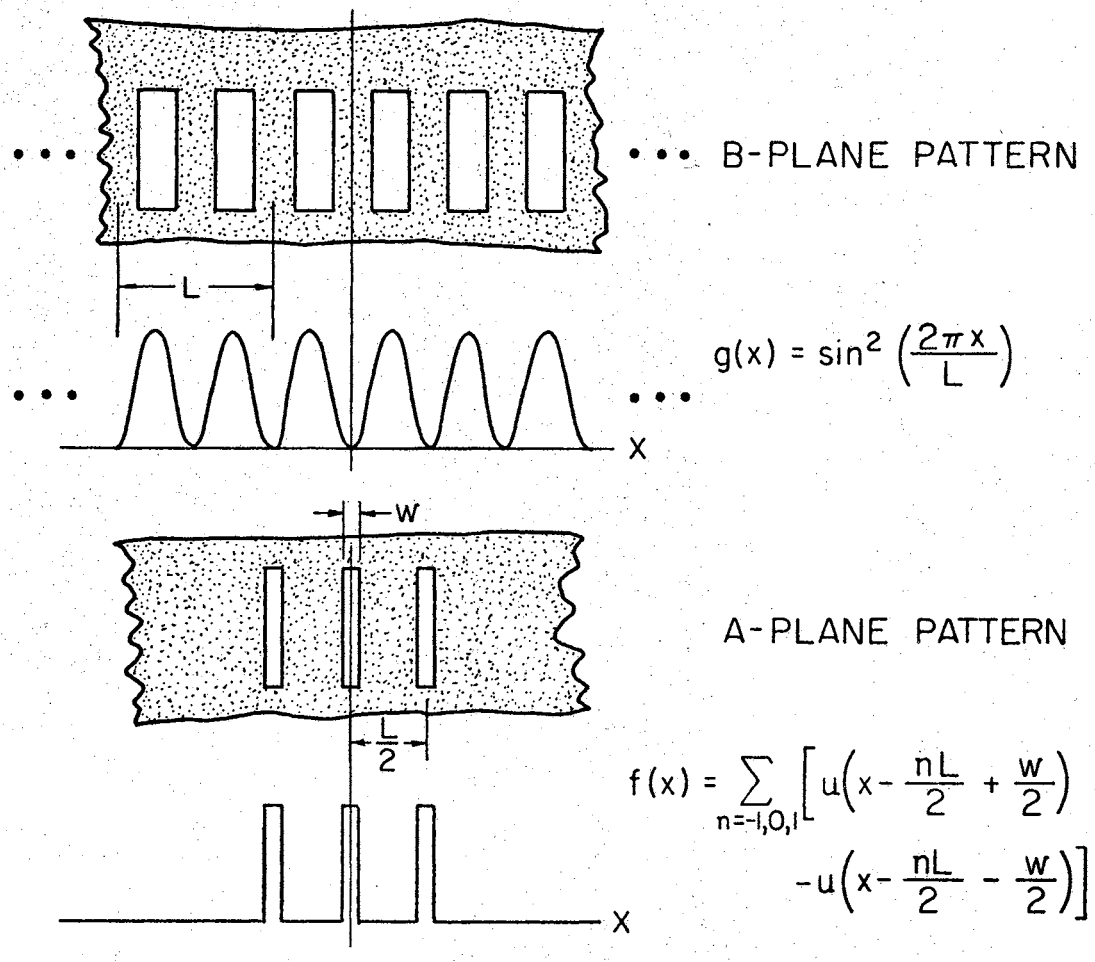

Figure 18. Images and Functions Used in Experiment Three

the A-plane and B-plane stripes can be expected to produce markedly different results.

Experiment Four

The A-plane and B-plane patterns for the fourth experiment are shown in Figure 20. The B-plane pattern is identical to the B-plane patterns used in the first three experiments. The A-plane pattern consists of two narrow stripes having four-thirds the spacing of the B-

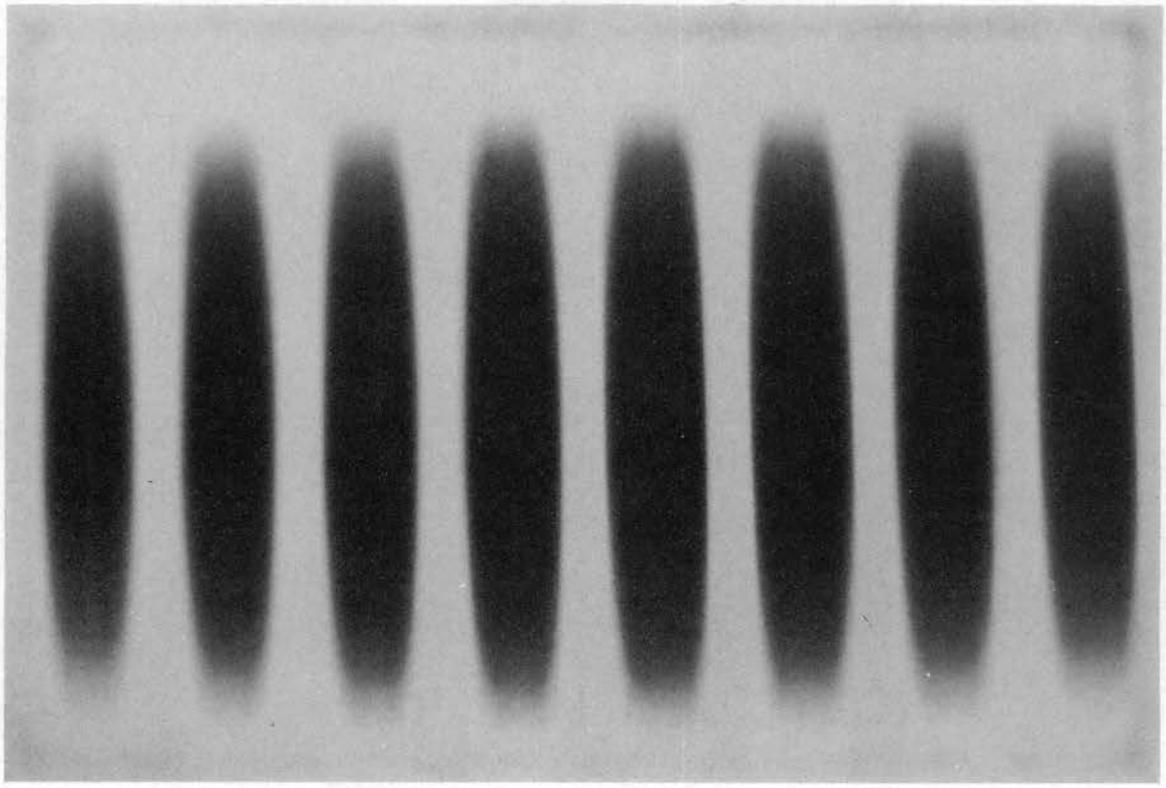

Figure 19. Cross-Correlation Results of Experiment Three

plane stripes.

The cross-correlation function may be determined in a manner similar to that for the case of two A-plane stripes considered previously. Again, as in Equation (5-1),

$$\rho(\alpha) = \int_{-\infty}^{\infty} f(x)\ g(x + \alpha)\ dx \quad ,$$

and for this particular case

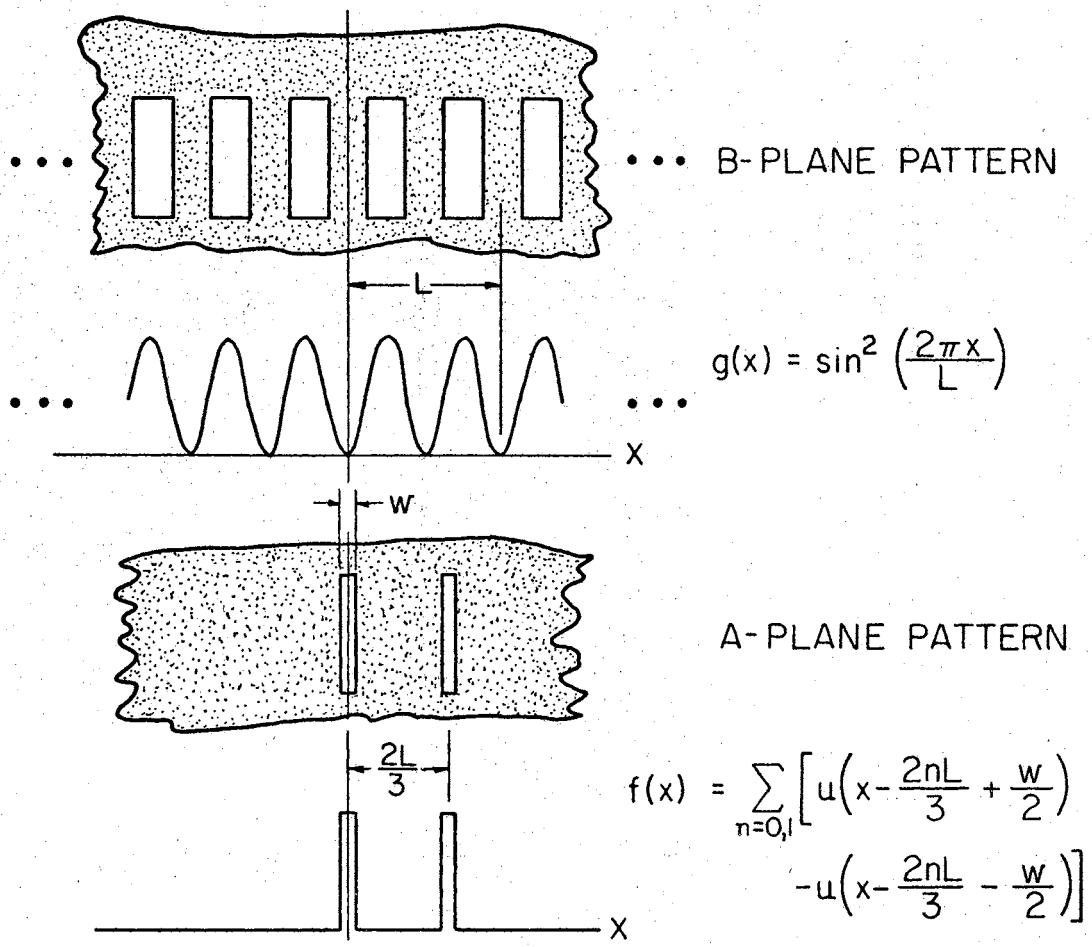

Figure 20. Images and Functions Used in Experiment Four

$$\rho(\alpha) = \int_{-a}^{a} \left[u(x + \tfrac{w}{2}) - u(x - \tfrac{w}{2}) + u(x - \tfrac{2L}{3} + \tfrac{w}{2}) - u(x - \tfrac{2L}{3} - \tfrac{w}{2})\right] \cdot \sin^2 \tfrac{2\pi}{L}(x + \alpha)\, dx \,, \tag{5-18}$$

where the limits of integration are chosen sufficiently large to include the entire domain of the function f(x). Then

$$\rho(\alpha) = \int_{-\frac{w}{2}}^{\frac{w}{2}} \sin^2 \frac{2\pi}{L}(x + \alpha)\, dx + \int_{\frac{2L}{3} - \frac{w}{2}}^{\frac{2L}{3} + \frac{w}{2}} \sin^2 \frac{2\pi}{L}(x + \alpha)\, dx, \quad (5\text{-}19)$$

and again, as developed previously, but with appropriate limits,

$$\rho(\alpha) = \tfrac{1}{2}\left[x - \frac{L}{4\pi} \sin \frac{4\pi}{L}(x + \alpha)\right]_{-\frac{w}{2}}^{\frac{w}{2}} + \tfrac{1}{2}\left[x - \frac{L}{4\pi}\sin \frac{4\pi}{L}(x + \alpha)\right]_{\frac{2L}{3} - \frac{w}{2}}^{\frac{2L}{3} + \frac{w}{2}} . \quad (5\text{-}20)$$

Evaluation of the above expression yields

$$\rho(\alpha) = \tfrac{1}{2}\left[\frac{w}{2} - \frac{L}{4\pi} \sin \frac{4\pi}{L}(\frac{w}{2} + \alpha) + \frac{w}{2} + \frac{L}{4\pi} \sin \frac{4\pi}{L}(\alpha - \frac{w}{2})\right] + \tfrac{1}{2}\left[(\frac{2L}{3} + \frac{w}{2})\right. \quad (5\text{-}21)$$

$$\left. - \frac{L}{4\pi} \sin \frac{4\pi}{L}(\alpha + \frac{w}{2} + \frac{2L}{3}) - (\frac{2L}{3} - \frac{w}{2}) + \frac{L}{4\pi} \sin \frac{4\pi}{L}(\alpha - \frac{w}{2} + \frac{2L}{3})\right] ,$$

which further reduces to

$$\rho(\alpha) = \tfrac{1}{2}\left\{w - \frac{L}{4\pi}\left[\sin \frac{4\pi}{L}(\alpha + \frac{w}{2}) - \sin \frac{4\pi}{L}(\alpha - \frac{w}{2})\right]\right\} \quad (5\text{-}22)$$

$$+ \tfrac{1}{2}\left\{w - \frac{L}{4\pi}\left[\sin \frac{4\pi}{L}(\alpha + \frac{w}{2} + \frac{2L}{3}) - \sin \frac{4\pi}{L}(\alpha - \frac{w}{2} + \frac{2L}{3})\right]\right\} .$$

For purposes of simplification, the above equation may be written as

$$\rho(\alpha) = \rho_1(\alpha) + \rho_2(\alpha) \quad (5\text{-}23)$$

where

$$\rho_1(\alpha) = \tfrac{1}{2}\left\{w - \frac{L}{4\pi}\left[\sin\frac{4\pi}{L}(\alpha + \frac{w}{2}) - \sin\frac{4\pi}{L}(\alpha - \frac{w}{2})\right]\right\}, \qquad (5\text{-}24)$$

and

$$\rho_2(\alpha) = \tfrac{1}{2}\left\{w - \frac{L}{4\pi}\left[\sin\frac{4\pi}{L}(\alpha + \frac{w}{2} + \frac{2L}{3}) - \sin\frac{4\pi}{L}(\alpha - \frac{w}{2} + \frac{2L}{3})\right]\right\}. \qquad (5\text{-}25)$$

Equation (5-24) may be simplified in the same manner as was Equation (5-4a) to yield

$$\rho_1(\alpha) \approx w\left[\sin^2(2\pi\frac{\alpha}{L})\right]. \qquad (5\text{-}26)$$

Use of the substitution

$$\phi = \alpha + \frac{2L}{3} \qquad (5\text{-}27)$$

in Equation (5-25) yields

$$\rho_2(\alpha) = \tfrac{1}{2}\left\{w - \frac{L}{4\pi}\left[\sin\frac{4\pi}{L}(\phi + \frac{w}{2}) - \sin\frac{4\pi}{L}(\phi - \frac{w}{2})\right]\right\}. \qquad (5\text{-}28)$$

This expression has the same form as that of Equation (5-24). Hence in view of Equation (5-26), it is seen that

$$\rho_2(\alpha) \approx w\left[\sin^2\frac{2\pi}{L}(\alpha + \frac{2L}{3})\right]. \qquad (5\text{-}29)$$

Use of Equations (5-26) and (5-29) in Equation (5-23) yields

$$\rho(\alpha) \approx w\left[\sin^2\left(\frac{2\pi\alpha}{L}\right) + \sin^2\left(\frac{2\pi\alpha}{L} + \frac{4\pi}{3}\right)\right] , \qquad (5\text{-}30)$$

or alternatively,

$$\rho(\alpha) \approx w\left[\sin^2\left(\frac{2\pi\alpha}{L}\right) + \sin^2\left(\frac{2\pi\alpha}{L} - \frac{2\pi}{3}\right)\right] . \qquad (5\text{-}31)$$

It was previously noted that the stripes in the B-plane pattern have been approximated mathematically by a simple sine-squared function. These patterns are more accurately represented by a square-wave pattern, which necessarily requires the inclusion of the higher-order odd harmonics to improve the mathematical representation. The associated increased complexity of the more accurate mathematical analysis can be alleviated by the use of graphical techniques. Figure 21 shows the same information shown in Figure 20, except that the B-plane transparency function is more accurately portrayed by its square-wave representation. Figure 22 illustrates the graphical processes used to develop and represent the theoretically predicted C-plane intensity function, which should be a more accurate analytical prediction than that given by Equation (5-31).

The corresponding experimental results obtained in the fourth experiment are shown in Figure 23. As may be seen in the first experiment, the resultant pattern shown in Figure 15 could be represented as a square-wave function with spatial frequency equal to that of the sine-squared function in Equation (5-7). If the two parts of Equation (5-31) are first represented as square-wave functions and subsequently added graphically as shown in Figure 22, the resultant sum predicts closely the function obtained in Figure 23. It is seen that the most

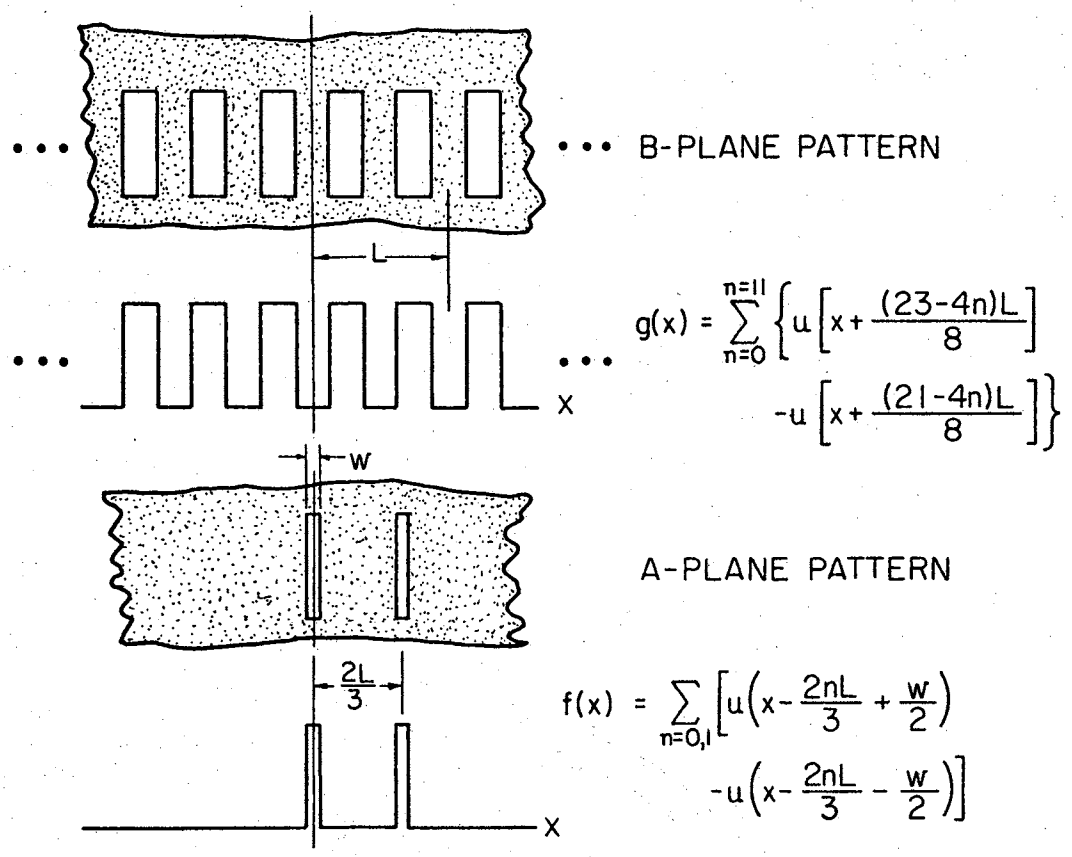

$$g(x) = \sum_{n=0}^{n=11} \left\{ u\left[x + \frac{(23-4n)L}{8}\right] - u\left[x + \frac{(21-4n)L}{8}\right] \right\}$$

$$f(x) = \sum_{n=0,1} \left[u\left(x - \frac{2nL}{3} + \frac{w}{2}\right) - u\left(x - \frac{2nL}{3} - \frac{w}{2}\right) \right]$$

Figure 21. Images and Functions Used for Graphical Analysis in Experiment Four

darkened parts of the photograph are the doubly-intense stripes of width L/12, spaced L/2 apart between centers, centered as pedestals on "plateau" or "butte" stripes which have single-unit intensity and have widths 5L/12, and are spaced L/2 apart between centers. Thus, the experimental result obtained is in reasonably good agreement with the graphically derived theoretical prediction. The experimental result is not well represented by the analytical approximation defined by Equation (5-31), since Equation (5-31) represents, essentially, a constant

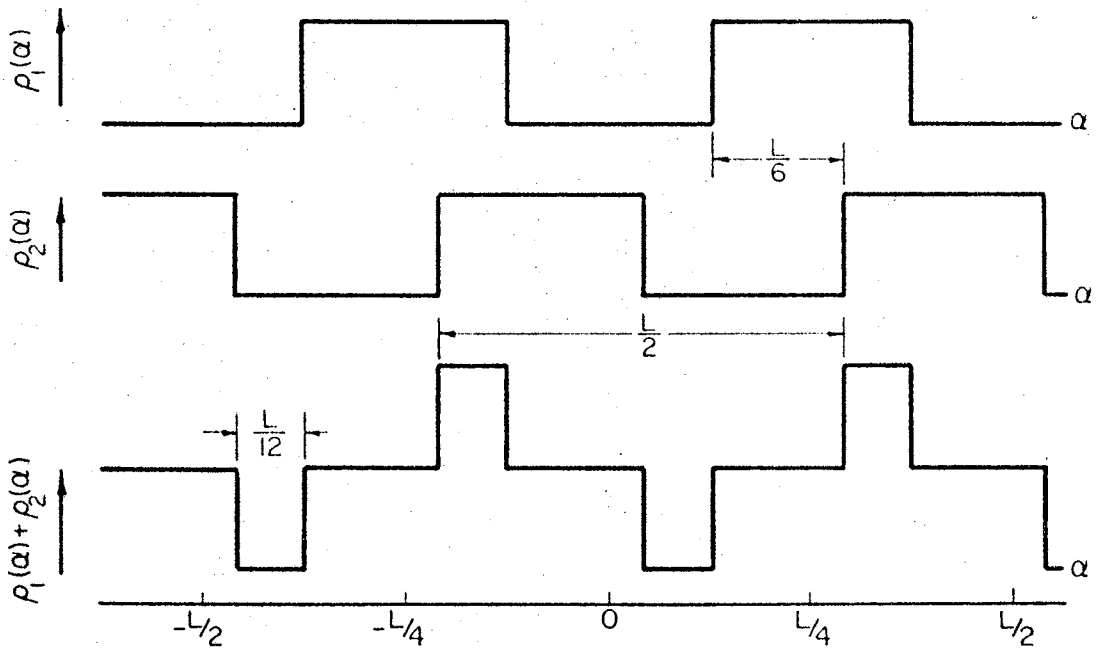

Figure 22. Graphical Construction of Predicted Intensity Function for Experiment Four

term plus the sum of two equal-period sine functions, and does not include the contributions of the higher harmonics needed to more-accurately portray the C-plane intensity function.

A repetition of this fourth experiment, with the single exception of making the spacing between the A-plane stripes 4L/3 instead of 2L/3, produced a nearly identical photographic result. This outcome could have been anticipated from the nature of Equation (5-31) and Figure 22.

Experiment Five

For the case depicted in Figure 24, and for the f(x) and g(x) functions assumed, the cross correlation function may be written as

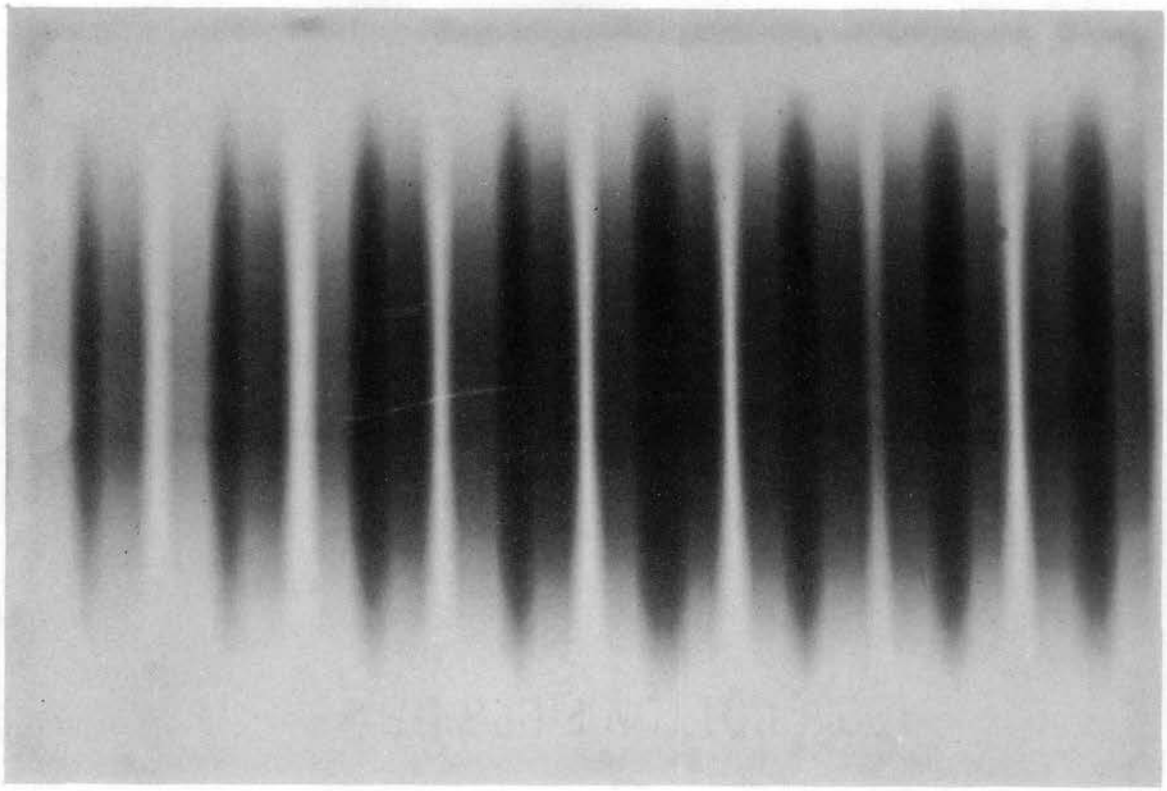

Figure 23. Cross-Correlation Results of Experiment Four

$$\rho(\alpha) = \int_{-a}^{a} \sum_{n=-1,0,1} \left[u(x - \frac{2nL}{3} + \frac{w}{2}) - u(x - \frac{2nL}{3} - \frac{w}{2}) \right] \cdot \sin^2 \frac{2\pi}{L}(x + \alpha) \; dx \qquad (5\text{-}33)$$

where as in the previous case the limits on the integral are sufficiently large. Then

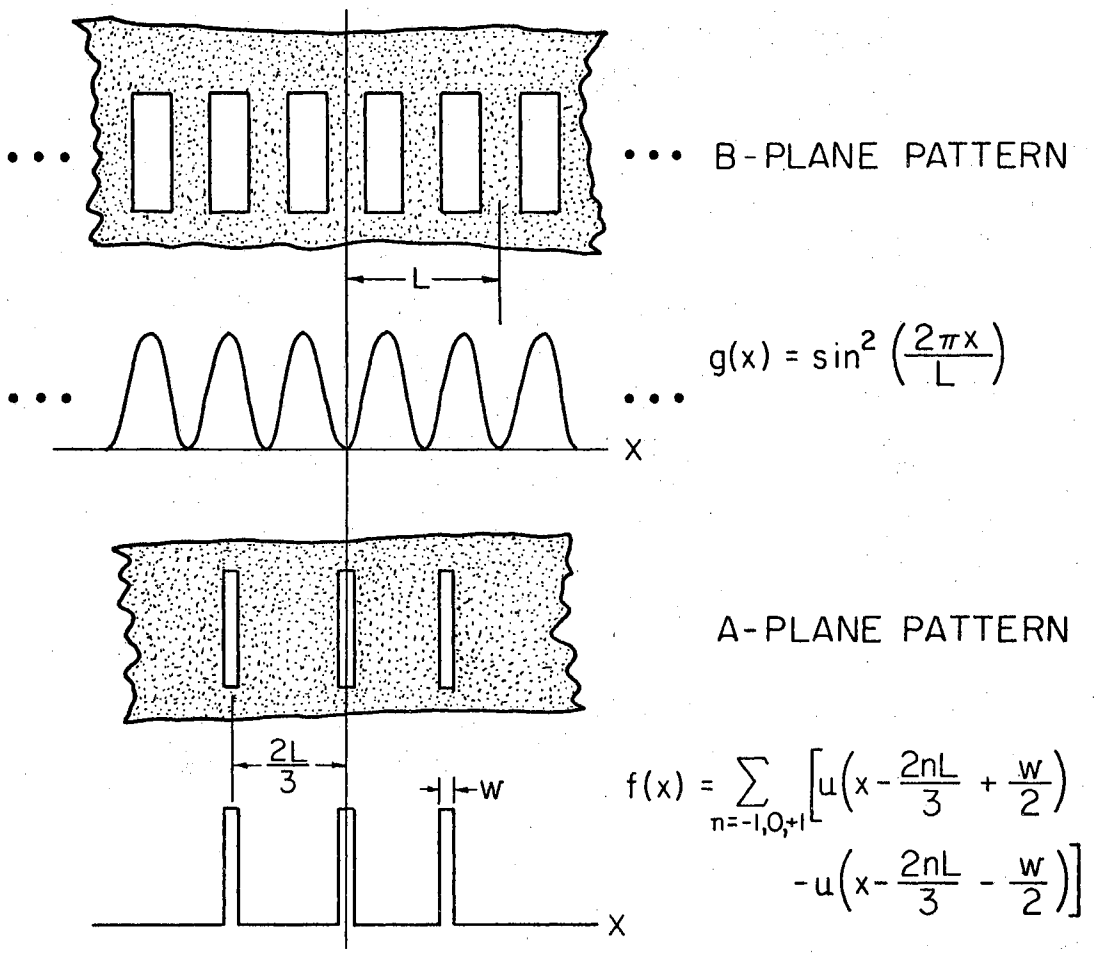

Figure 24. Images and Functions Used in Experiment Five

$$\rho(\alpha) = \int_{-\frac{2L}{3}-\frac{w}{2}}^{-\frac{2L}{3}+\frac{w}{2}} \sin^2 \frac{2\pi}{L}(x+\alpha)\, dx + \int_{-\frac{w}{2}}^{\frac{w}{2}} \sin^2 \frac{2\pi}{L}(x+\alpha)\, dx \tag{5-34}$$

$$+ \int_{\frac{2L}{3}-\frac{w}{2}}^{\frac{2L}{3}+\frac{w}{2}} \sin^2 \frac{2\pi}{L}(x+\alpha)\, dx \quad .$$

Integrating with respect to x and evaluating at the limits yields

$$\rho(\alpha) = \tfrac{1}{2}\left\{w - \frac{L}{4\pi}\left[\sin\frac{4\pi}{L}(\alpha + \frac{w}{2} - \frac{2L}{3}) - \sin\frac{4\pi}{L}(\alpha - \frac{w}{2} - \frac{2L}{3})\right]\right\}$$
$$+ \tfrac{1}{2}\left\{w - \frac{L}{4\pi}\left[\sin\frac{4\pi}{L}(\alpha + \frac{w}{2}) - \sin\frac{4\pi}{L}(\alpha - \frac{w}{2})\right]\right\} \qquad (5\text{-}35)$$
$$+ \tfrac{1}{2}\left\{w - \frac{L}{4\pi}\left[\sin\frac{4\pi}{L}(\alpha + \frac{w}{2} + \frac{2L}{3}) - \sin\frac{4\pi}{L}(\alpha - \frac{w}{2} + \frac{2L}{3})\right]\right\} .$$

For simplification purposes the above equation may be written as

$$\rho(\alpha) = \rho_3(\alpha) + \rho_1(\alpha) + \rho_2(\alpha) \qquad (5\text{-}36)$$

where if

$$\rho_3(\alpha) = \tfrac{1}{2}\left\{w - \frac{L}{4\pi}\left[\sin\frac{4\pi}{L}(\alpha + \frac{w}{2} - \frac{2L}{3}) - \sin\frac{4\pi}{L}(\alpha - \frac{w}{2} - \frac{2L}{3})\right]\right\} . \qquad (5\text{-}37)$$

$\rho_1(\alpha)$ and $\rho_2(\alpha)$ are then defined in Equations (5-24) and (5-25) respectively. If, in the manner of Equation (5-24), the definition

$$\theta \equiv \alpha - \frac{2L}{3} \qquad (5\text{-}38)$$

is made, then substituting θ above into Equation (5-36) yields

$$\rho_3(\alpha) = \tfrac{1}{2}\left\{w - \frac{L}{4\pi}\left[\sin\frac{4\pi}{L}(\theta + \frac{w}{2}) - \sin\frac{4\pi}{L}(\theta - \frac{w}{2})\right]\right\} \qquad (5\text{-}39)$$

which can be simplified in the same manner as Equation (5-29) to yield

$$\rho_3(\alpha) \approx w\left[\sin^2\frac{2\pi}{L}(\alpha - \frac{2L}{3})\right] . \qquad (5\text{-}40)$$

From Equation (5-36) and the respective constituent equations, (5-40), (5-24) and (5-25), the following may be written

$$\rho(\alpha) \propto \left[\sin^2\left(\frac{2\pi\alpha}{L} - \frac{4\pi}{3}\right) + \sin^2\left(\frac{2\pi\alpha}{L}\right) + \sin^2\left(\frac{2\pi\alpha}{L} + \frac{4\pi}{3}\right)\right], \quad (5\text{-}41)$$

Equation (5-41) shows three terms with distinct arguments compared to two in Equation (5-31) for the fourth experiment. If a square-wave function were presumed for each of the sine-squared terms in Equation (5-41), a graphical addition could be performed as before to yield a square-wave predicted intensity function. The graphical analysis shown in Figure 25 is similar to that in Figure 22 except that the finite slope of the sides of each of the geometric wave functions is shown. The effect of the stripe width w in these wave functions may be determined from Equation (4-14) and the discussion preceding it. Figure 25 shows first the addition required to obtain the function predicted for the fourth experiment (middle) when stripe width w is considered. Then the function $\rho_3(\alpha)$ is added to obtain the predicted intensity function for Experiment Five (bottom). It should be noted that this predicted function has a spatial frequency greater than that of the constituent A-plane and B-plane functions in contrast to the same spatial frequency predicted and observed in the third experiment. The predicted function for this experiment also has only two definite levels of intensity in contrast to the case of the fourth experiment.

The corresponding experimental results are shown in Figure 26. These results again appear to be in good agreement with those predicted by use of Equation (5-41) and the graphical interpretation of Figure 25. It should be noted again that use of Equation (5-41) without the aid of

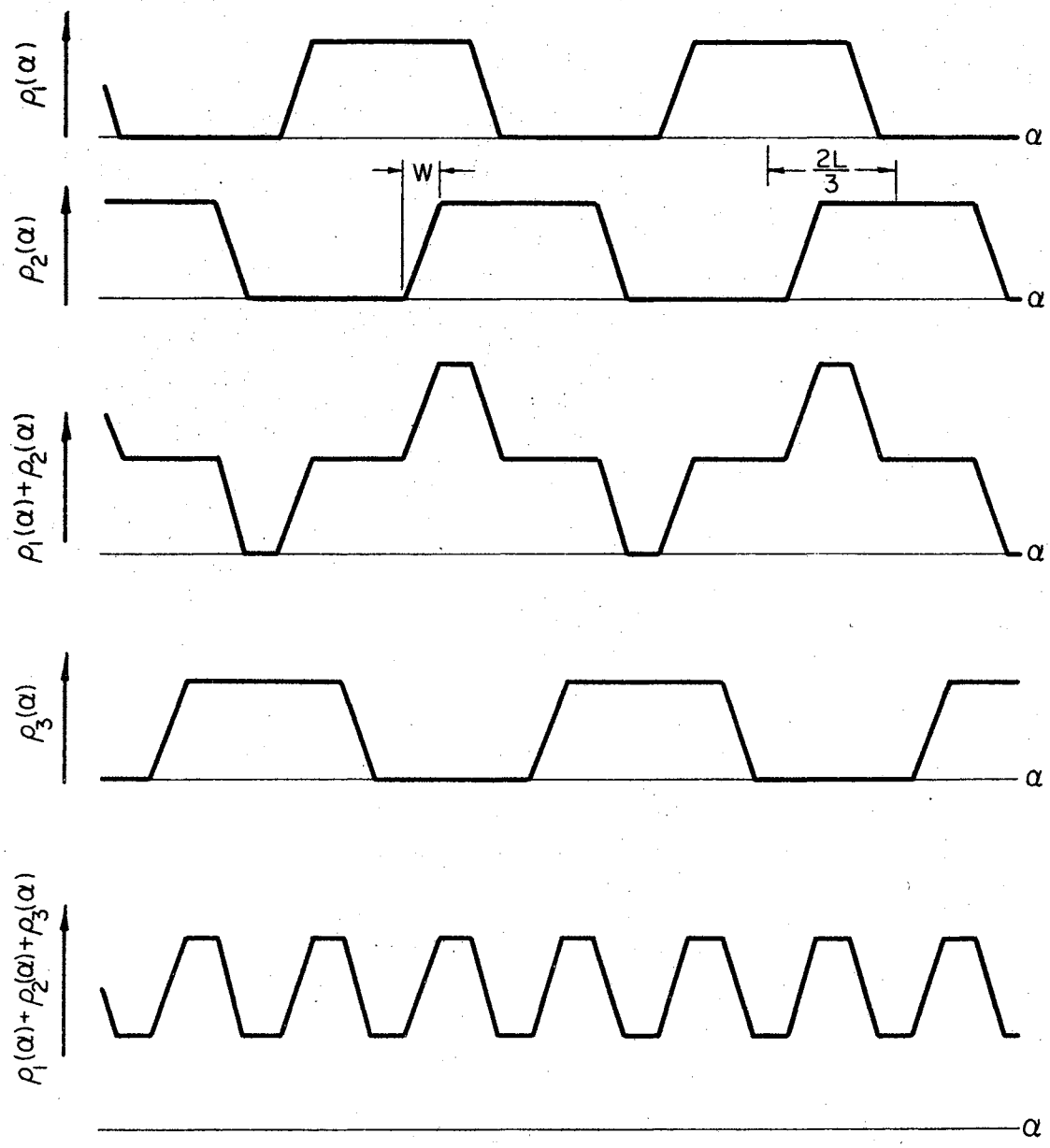

Figure 25. Graphical Construction of Predicted Intensity Function for Experiment Five

graphical interpretation or computation with higher harmonics would not yield the spatial frequency characteristic observed.

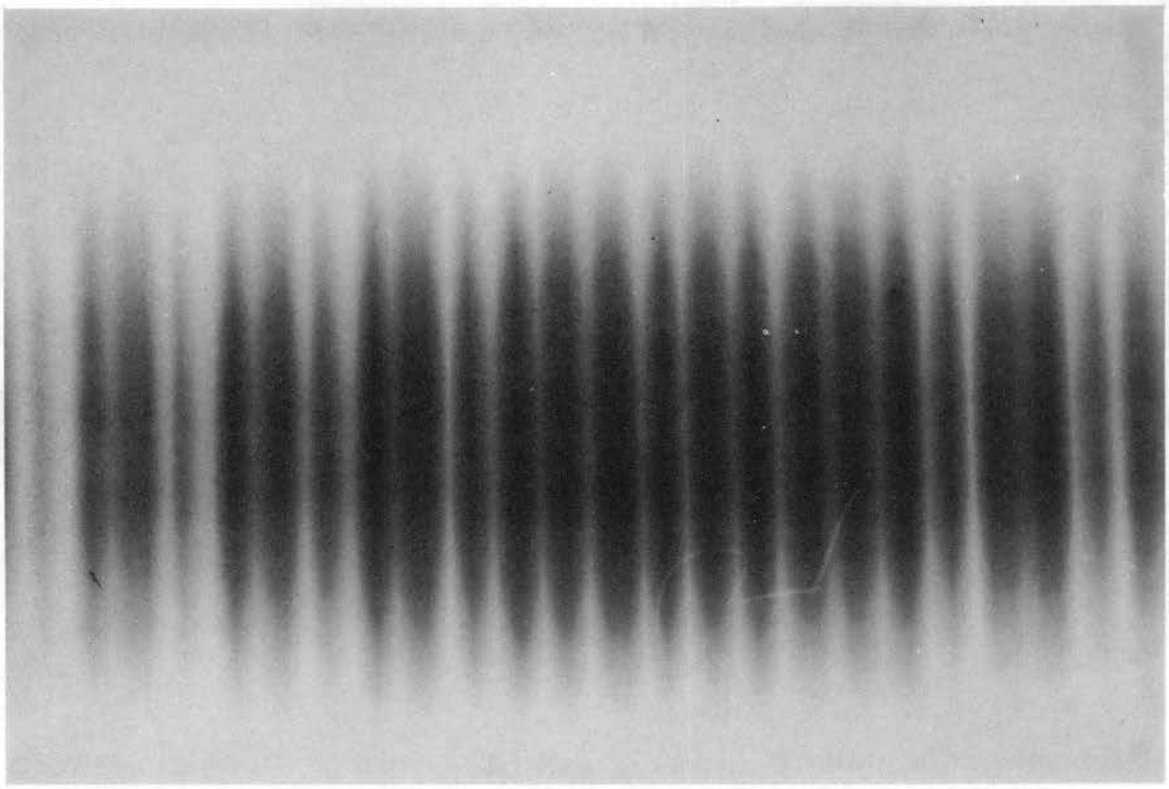

Figure 26. Cross-Correlation Results of Experiment Five

CHAPTER VI

PATTERN ORIENTATION EXPERIMENTS

Considerable information concerning orientation of predominant characteristics of patterns may be obtained with the optical cross correlator by making one of the patterns a single narrow stripe with adjustable orientation. This operation provides increased insight into the application possibilities of the optical cross-correlation technique.

A single narrow stripe centered on a 360° protractor was chosen for the A-plane pattern in the following experiments. The protractor was edge-mounted in a larger sheet of plastic which was cut to the dimensions of the A-plane transparencies used previously. The protractor was mounted snugly in the encircling plastic and provided with an index mark, so that the transparent stripe on the protractor could be positioned at any desired angle relative to the vertical axis. Again, the experimental correlation functions were recorded directly on the photographic paper so that areas of low intensity correspond to light or white while higher intensity areas correspond to darker or black areas. A lighter area is noticeable in the center of the cross-correlation records of several of the figures for the following experiments. This was due to the increased diffusion and scattering of light from the center of the A-plane stripe caused by the center hole in the plastic protractor. This phenomenon, although noticeable, does not detract significantly from the experimental results obtained.

The approach for the following sequence of experiments was to progress from simple patterns to those of a more complex nature. Simpler patterns were studied initially so that their individual characteristics could be recognized more easily when integrated into complex patterns.

Straight-Line Patterns

Figure 27 shows five cross-correlation records generated with the optical cross correlator and, in addition, a representation of the constituent patterns when the B-plane pattern consisted of a single vertical stripe. It may be noted that in this and subsequent figures the B-plane pattern representation was derived directly from the B-plane transparency used in the respective experiments. By use of this procedure the relative dimensions of the B-plane patterns and the cross correlation records were preserved. It may be seen from Figure 27 that the cross-correlation records graduate from maximum intensity for the A-plane stripe vertical to a minimum intensity for the A-plane stripe oriented horizontally.

The next experiment used the same A-plane pattern orientations used in the experiment depicted in Figure 27 except that the B-plane pattern comprised the series of wide vertical stripes used in the experiments of Chapter V. Figure 28 shows the results obtained. Since the A-plane stripe in this case is narrow with respect to the B-plane stripes, the graduation of intensity at the edges of the stripes in Figure 28 (a) is barely perceptible and the cross-correlation record appears to be a reproduction of the B-plane pattern.

Several observers have noted that the original cross-correlation record of Figure 28 (b) at certain viewing distances caused an instabil-

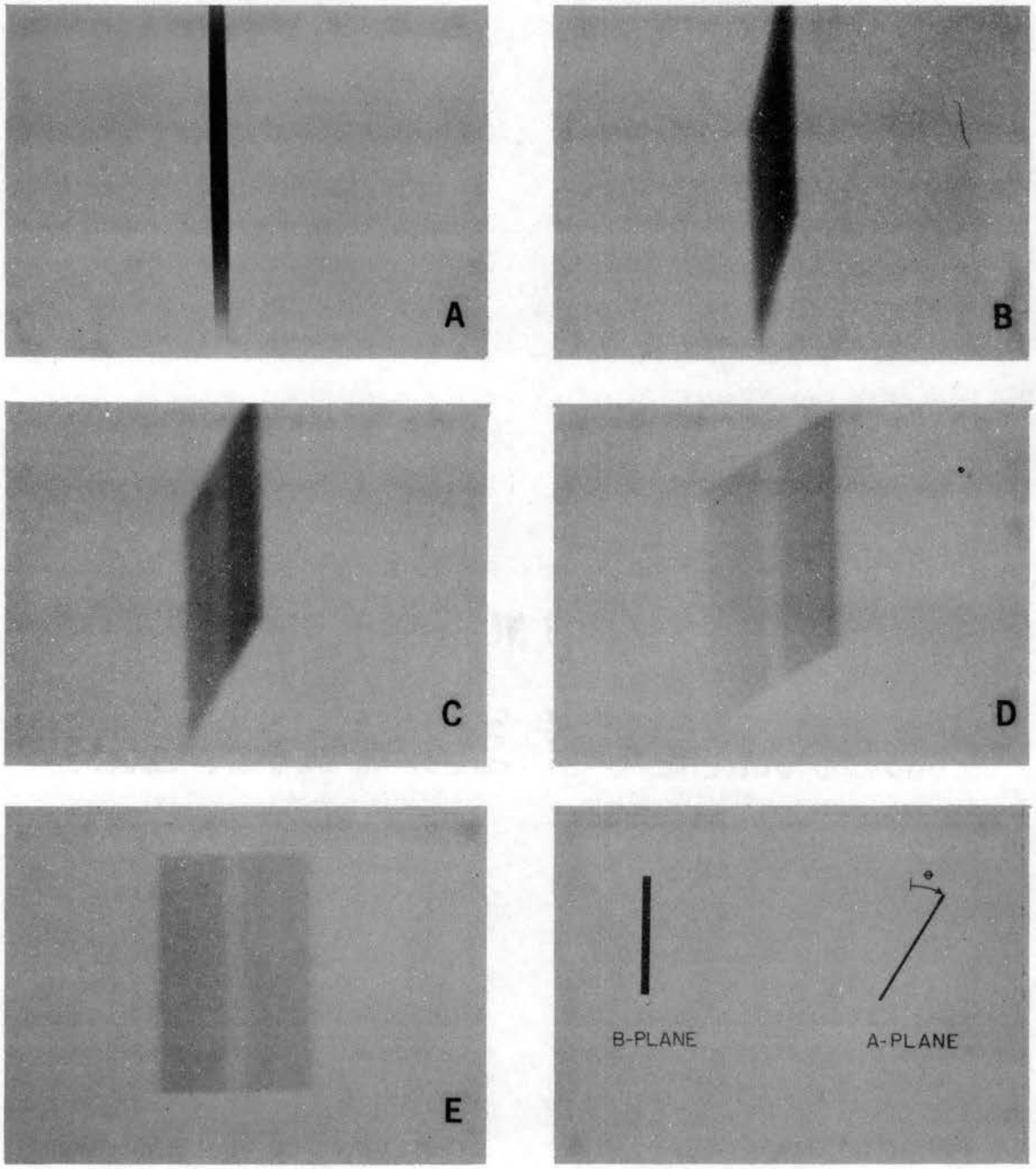

Figure 27. Cross Correlation Between a Single Wide Stripe and a Single Narrow Stripe Inclined at (a) 0, (b) 15, (c) 30, (d) 60 and (e) 90 Degrees

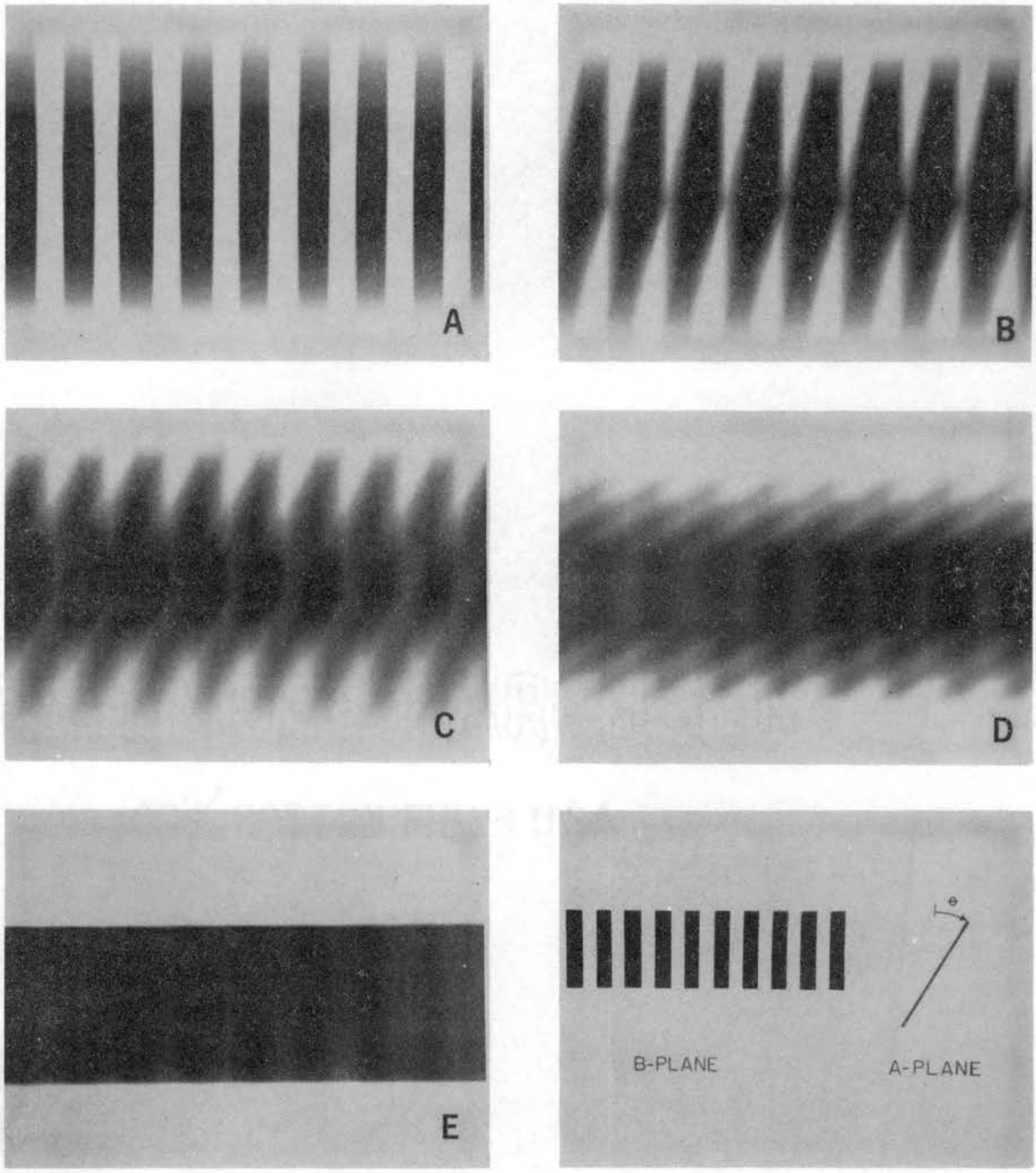

Figure 28. Cross Correlation Between a Series of Wide Stripes and a Single Narrow Stripe Inclined at (a) 0, (b) 15, (c) 30, (d) 60 and (e) 90 Degrees

ity or oscillation in their visual system. Rough estimates place the frequency of this phenomenon at less than 20 cps and greater than 2 cps. Although the matter was not pursued, the evidence of the 5-6 cps visual scanning mechanism mentioned by Blackwell (7) would seem to be supported by these observations.

An experiment to investigate the possibility of separating features of two dimensional patterns used a series of "inverted els" for an example of a pattern with two equal and distict features. The results of the experiment are shown in Figure 29. It may be seen that the vertical component of each character is detected as a more intense vertical stripe in the cross-correlation pattern. As before, the intensity of the pattern is significantly greater when the A-plane and B-plane patterns have the same orientation. Further, it may be seen that when the horizontal feature of the character sequence is considered the fact that the horizontal features of the individual characters are collinear results in a pattern with greater intensity than for the vertical case.

Figure 30 shows a set of cross-correlation patterns for a series of narrow stripes inclined at an angle of 30 degrees in the B-plane and the A-plane pattern described previously. The stripe spacing was uniform in the left-hand portion of the pattern while the spacing lacked uniformity in the right-hand portion. The choice of such a pattern was motivated by the desire to simulate some of the features of handwriting or hand printing. The narrow stripes yield a greater contrast or sensitivity to orientation than do the wide stripes as may be noted by comparison of the results in Figure 30 with those in Figure 28.

An effort to further simulate features characteristic of handwriting or hand printing led to the addition of horizontal lines or bars to a

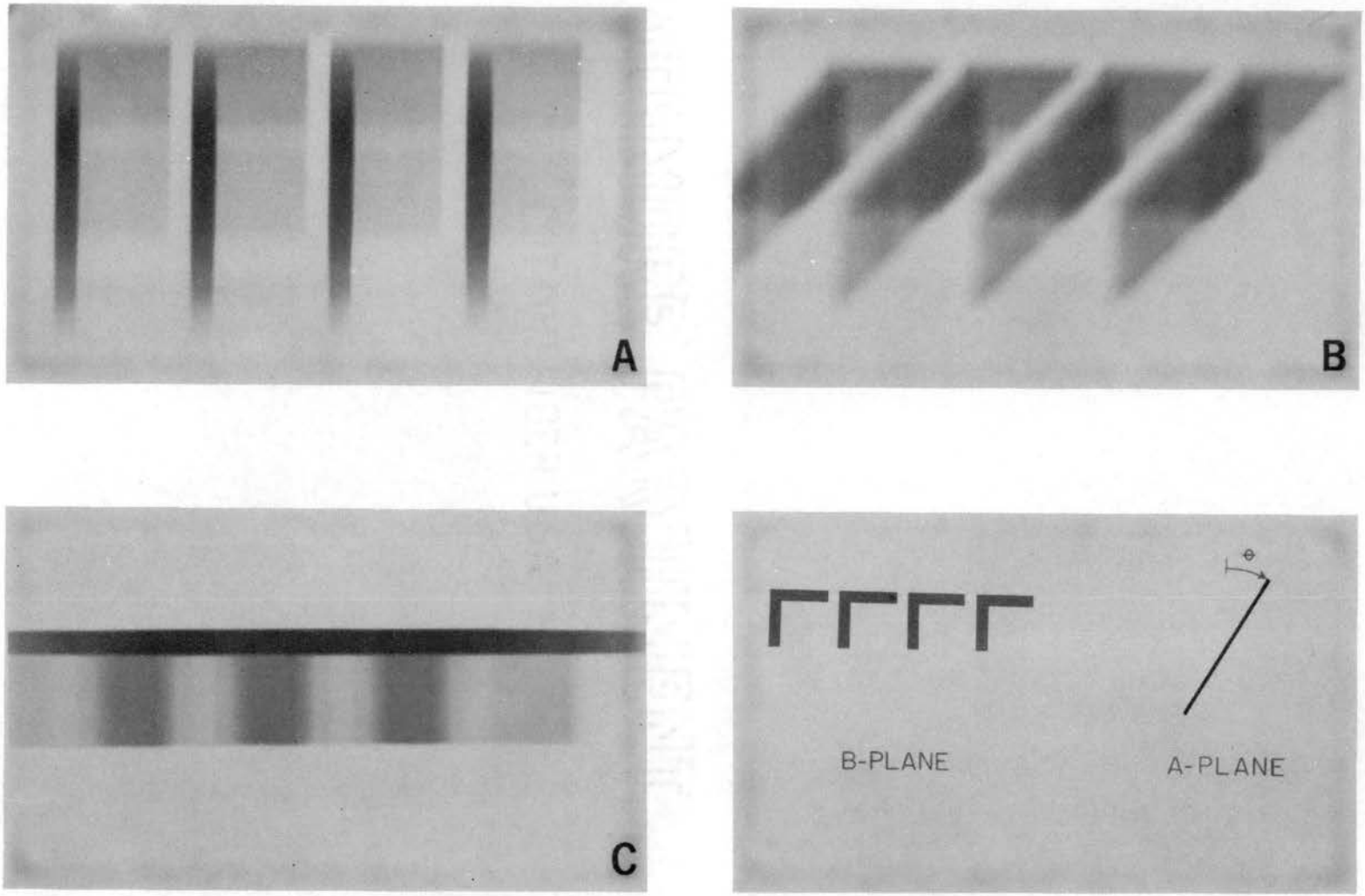

Figure 29. Cross Correlation Between a Series of "Inverted Els" and a Single Narrow Stripe Inclined at (a) 0, (b) 45 and (c) 90 Degrees

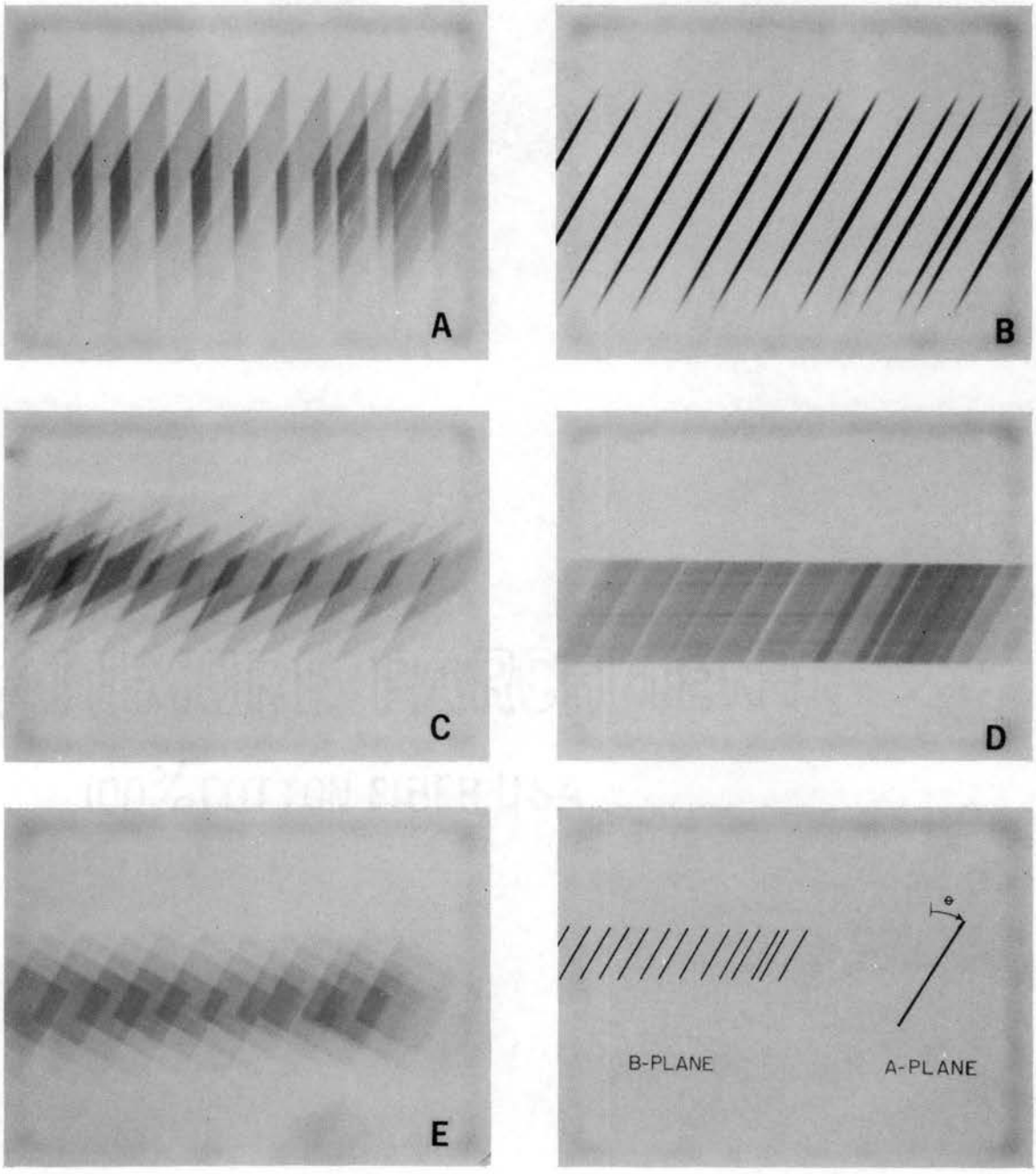

Figure 30. Cross Correlation Between a Series of Inclined Narrow Stripes and a Single Narrow Stripe Inclined at (a) 0, (b) 30, (c) 60, (d) 90 and (e) 120 Degrees

series of equally spaced narrow stripes or lines inclined 30 degrees with respect to the vertical. The continuous stripe at the base of the series of inclined stripes appeared to be more characteristic of handwriting than hand-printing from a subjective evaluation. Further discussion of the base-line feature is presented with subsequent experiments. Again, the results of Figure 31 show a distinct contrast in the cross-correlation patterns when the A-plane stripe was oriented similarly to components of the B-plane pattern. Further, Figure 31 (d) shows the effect of slight misalignment when the A-plane stripe was positioned at nominal horizontal or 90 degrees. The misalignment results in the slight separation of the ends of the more intense areas in the center of the cross-correlation record. These intense streaks correspond to the three short horizontal stripes in the B-plane pattern and would be collinear under conditions of ideal alignment.

Hand-Printed and Handwritten Patterns

Figure 32 shows the results of the first experiment in extracting straight line features from actual hand printed characters. In this experiment the number sequence "74074" was used in the B-plane and the variable-orientation stripe described previously was used in the A-plane. As may be noted, for the A-plane stripe vertical, the maximum correlation seems to come from the sides of the "0" (center) while a lesser correlation seems to exist for the other characters. When the A-plane stripe is oriented at or near the normal slant of the writing, the correlation pattern is dominated by the effects of the "vertical" or "slant axis" strokes of the characters. It may be noted that the correlation of the "0" is increased as might have been expected since it more nearly

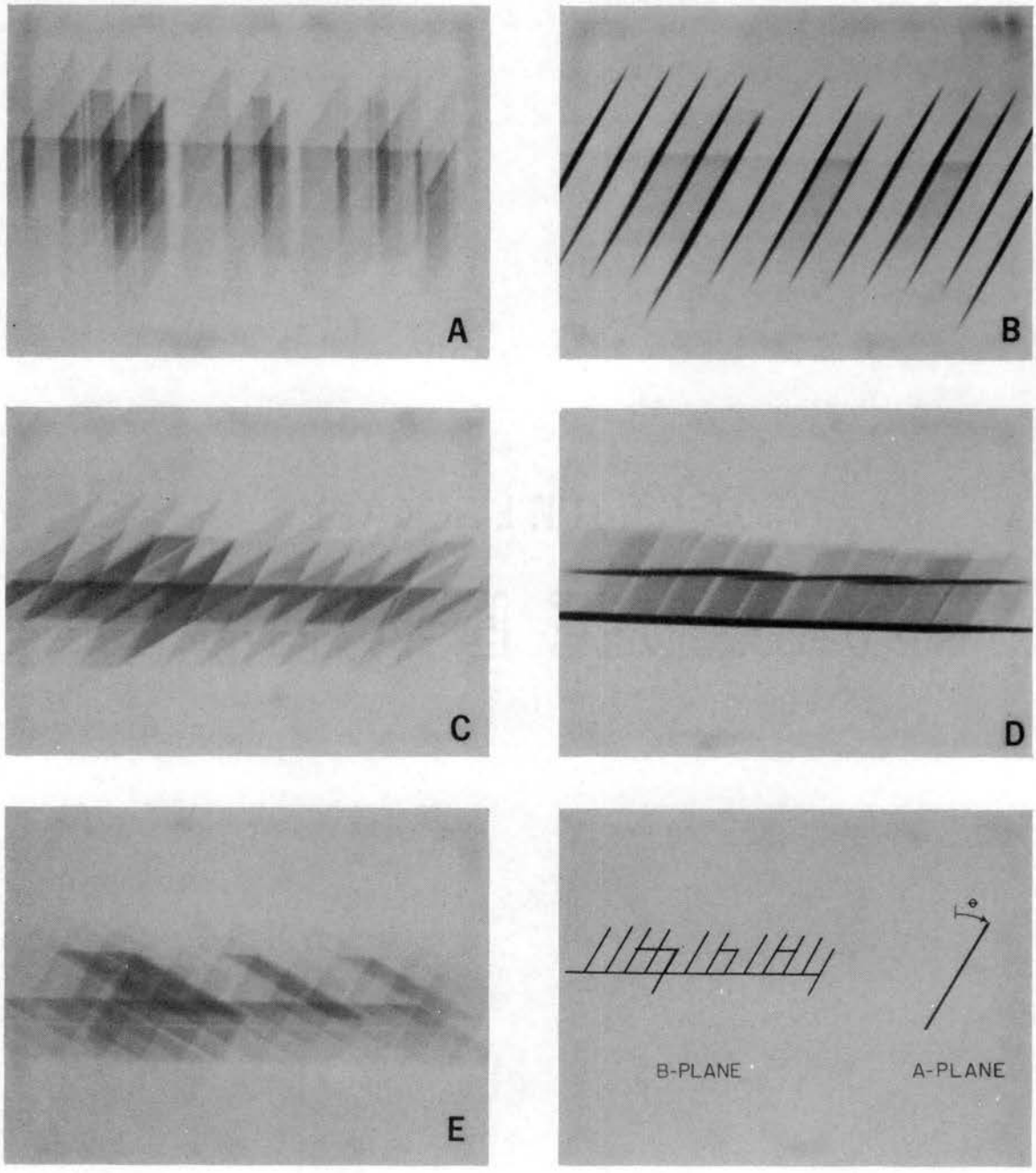

Figure 31. Cross Correlation Between a Series of Inclined Narrow Stripes With Some Horizontal Stripes and a Single Narrow Stripe Inclined at (a) 0, (b) 30, (c) 60, (d) 90 and (e) 120 Degrees

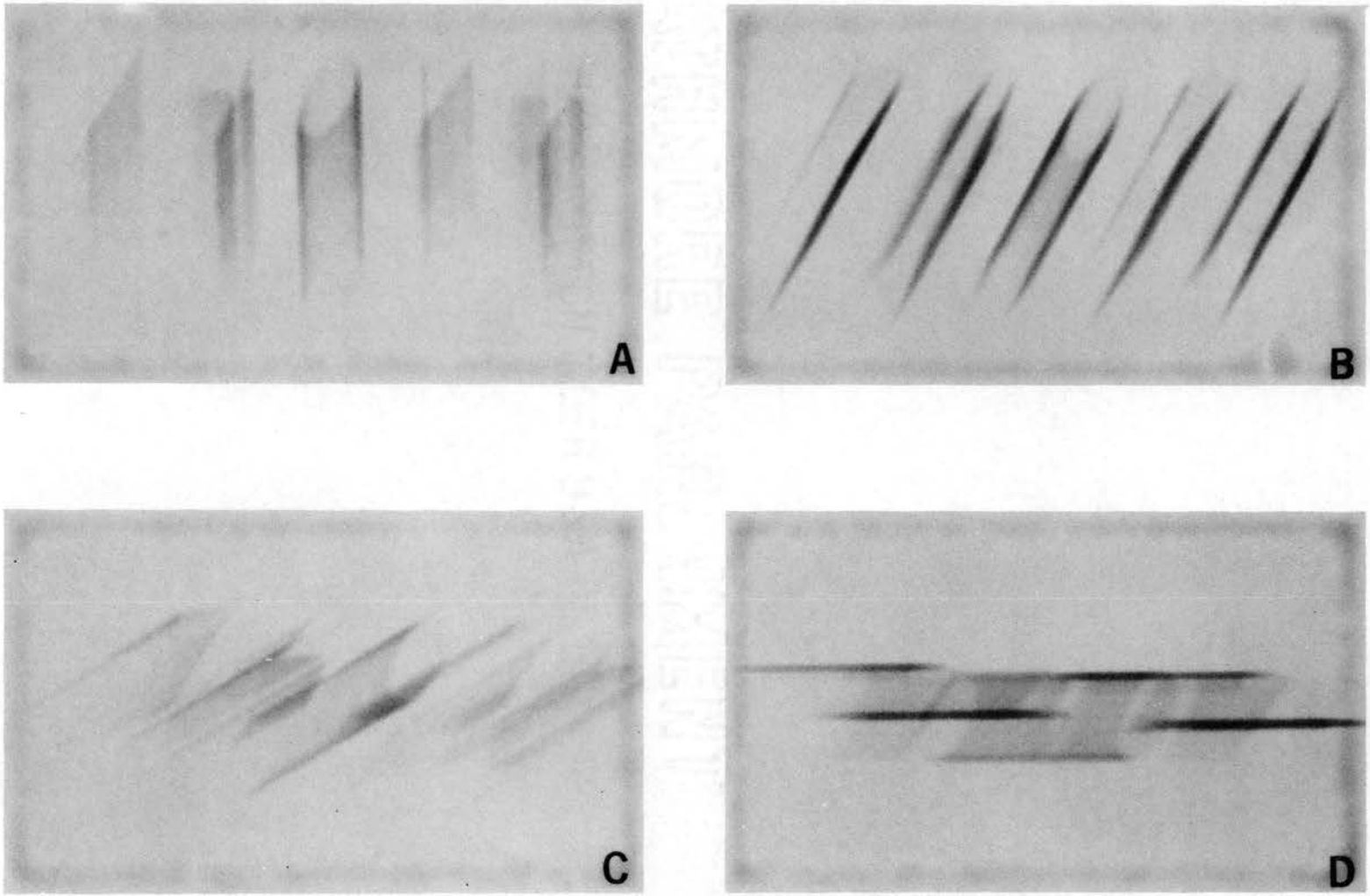

Figure 32. Cross Correlation Between the Hand-Printed Numerals "74074" and a Single Narrow Stripe Inclined at (a) 0, (b) 30, (c) 60 and (d) 90 Degrees

resembles an elipse with major axis coincident with the "slant axis" than it does a circle. For the A-plane stripe inclined at 60 degrees, the intensity of the correlation pattern diminished and again the sides of the "0" seemed to dominate. Figure 32 (d) shows the distinct separation of the horizontal features from others in the sequence of numbers. The stripes on the upper level in the cross-correlation record correspond to the high horizontal component of the "7" characters while the middle level stripes correspond to the intermediate-level horizontal component in the "4" characters. A lesser horizontal component from the "0" character may be seen on the two extreme levels.

An experiment using the handwritten word "fluid" was performed similarly to the previous experiments except that the average or predominant slant of the handwriting was determined by a subjective determination of maximum contrast in the C plane while the A-plane stripe orientation was varied. The maximum contrast or sharpness shown in Figure 33 (c) seemed to occur for an A-plane stripe orientation of 34 degrees. The results are barely distinguishable from those in Figure 33 (b) except for an increased intensity associated with the main stroke of the letter "f" at the extreme left side of the correlation pattern. A notable result of this experiment was the evidence of a predominant base line in the handwritten word when the A-plane stripe was horizontal. Although this characteristic was expected to some degree as mentioned earlier, Figure 33 (e) shows how this particular feature of a handwritten word was effectively separated from other features.

A second handwritten word was examined similarly to the previous one. The word "pattern" used in the latter experiment had greater line width and less uniformity than the previous word. The exposure time and

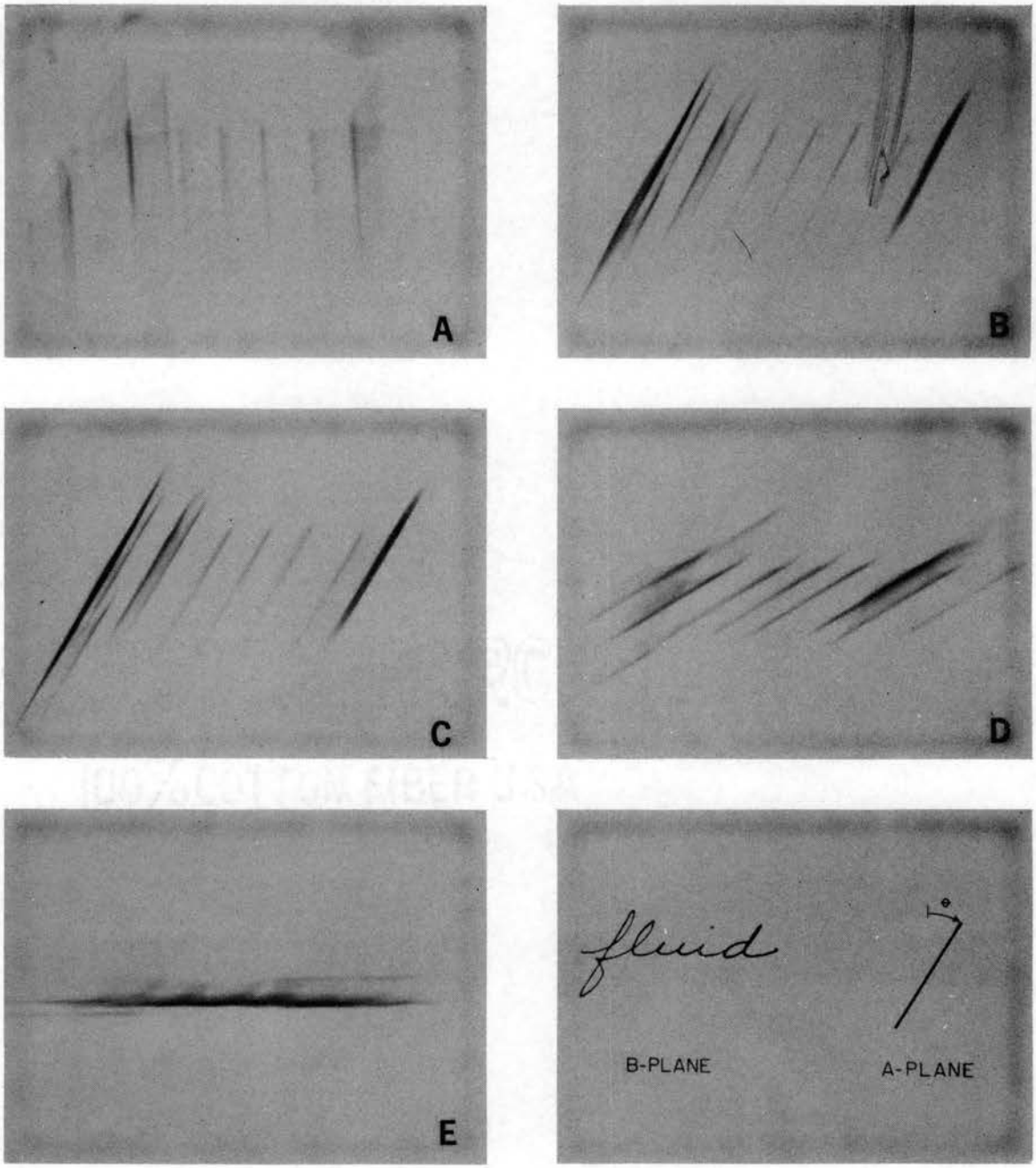

Figure 33. Cross Correlation Between the Handwritten Word "Fluid" and a Single Narrow Stripe Inclined at (a) 0, (b) 30, (c) 34, (d) 60, and (e) 90 Degrees

light source intensity were the same as used in the previous experiment and thus the greater width of the lines resulted in the more intense or darker cross-correlation patterns of Figure 34. A subjective determination of maximum contrast in the neighborhood of 30 degrees yielded an angle of slant of 26 degrees with respect to the vertical. Although the two handwriting samples were from the same subject, the congruity was as close as expected from the relatively coarse indexing and measurement system and subjective determination of contrast. A noticeable increase in line features oriented at 60 degrees with respect to the vertical is evident in Figure 34 (d) compared with those in Figure 33 (d) for the word "fluid."

A marked increase in complexity is observed in the pattern comprising a three-line address with some numbers. Figure 35 shows the cross-correlation patterns which resulted from the address shown and a single narrow stripe of variable orientation used in the previous experiments. Retention of the separation between words is evident in the cross-correlation record of Figure 35 (a) and for the top line at least in the two subsequent records. Figure 35 (b) shows the cross-correlation record for the case of maximum contrast which seemed to occur when the A-plane stripe was oriented at an angle of 27 degrees with respect to the vertical. It may be noted at this point that the handwritten address and the handwritten words in the two previous experiments were samples of handwriting from the same subject.

The difference between the records for the angle for maximum contrast and the record for 30 degrees in Figure 35 is difficult to distinguish. The record for an A-plane stripe orientation of 60 degrees shows two horizontal streaks of greater intensity which evidently result from

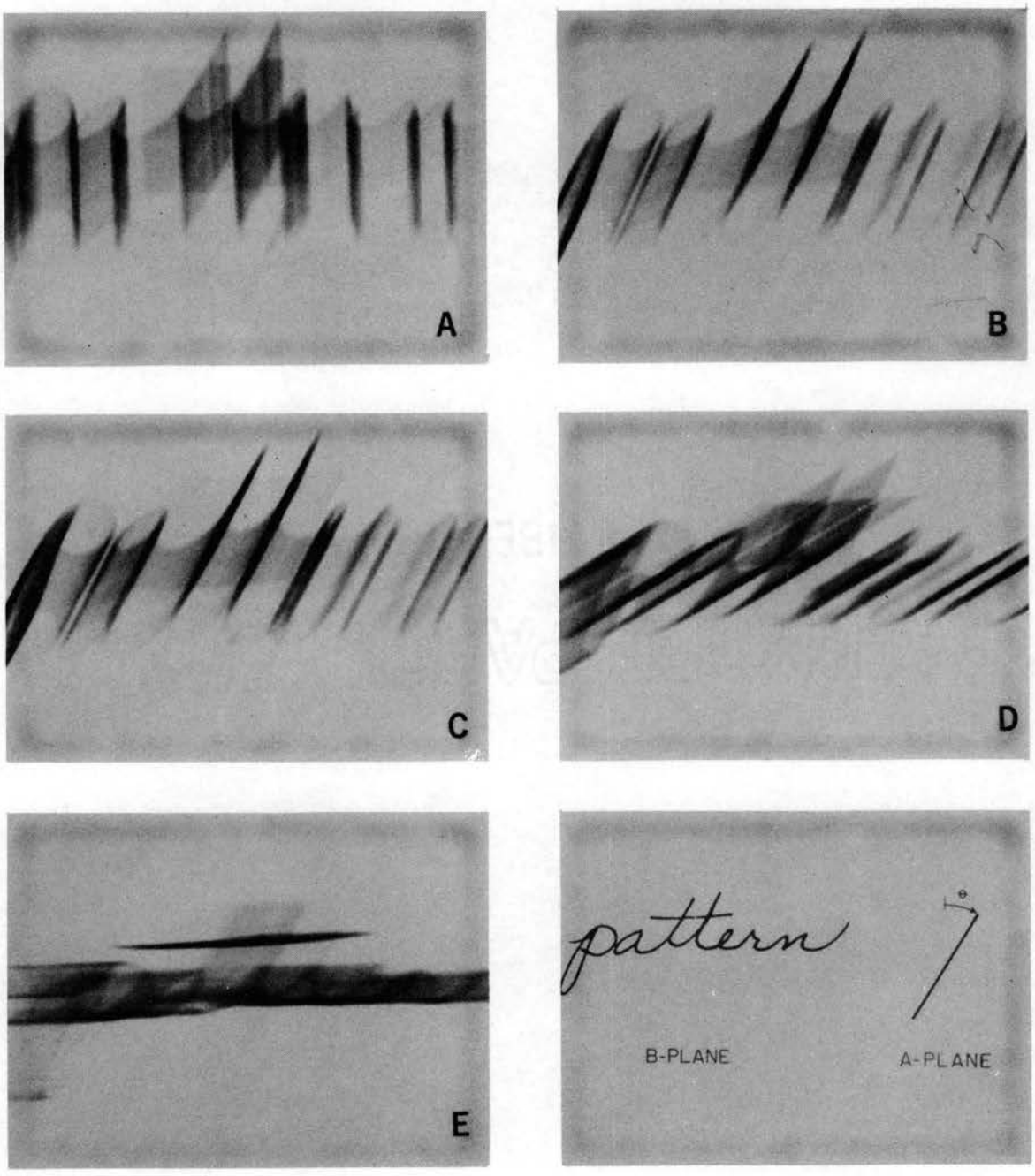

Figure 34. Cross Correlation Between the Handwritten Word "Pattern" and a Single Narrow Stripe Inclined at (a) 0, (b) 26, (c) 30, (d) 60 and (e) 90 Degrees

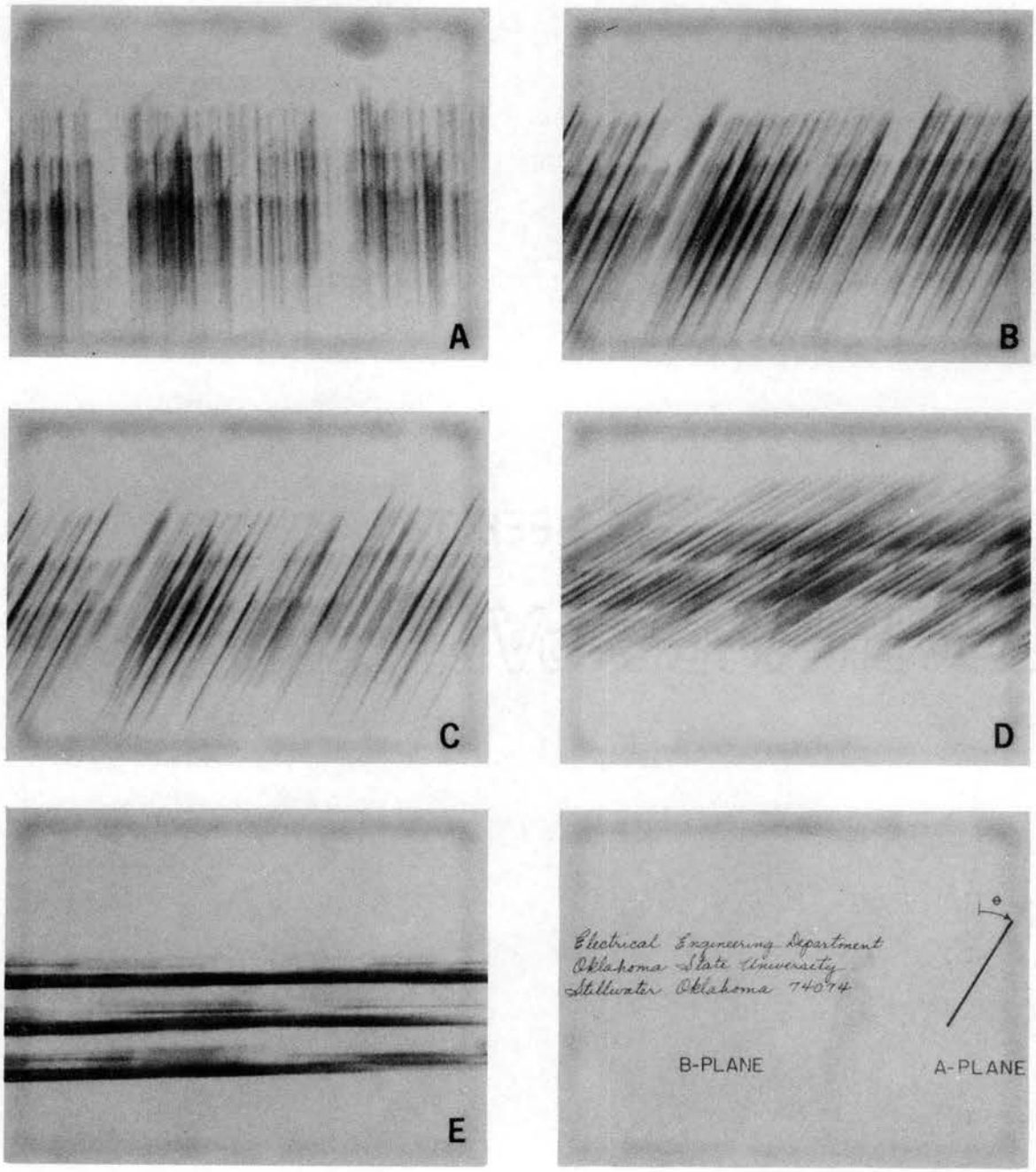

Figure 35. Cross Correlation Between a Handwritten Three-Line Address and a Single Narrow Stripe Inclined at (a) 0, (b) 27, (c) 30, (d) 60 and (e) 90 Degrees

the areas of overlap of the correlation patterns of the three lines. Probably most significant in the experiment was the demonstration of the separation of the individual lines of the three-line address. As in the case of the single handwritten words, a definite base line appears with a slightly less intense intermediate-level line corresponding to each line of the handwriting. The extreme right-hand end of the lower line in Figure 35 (e) shows that in the area of the numerals, the predominant base line did not appear and instead the horizontal line characteristics were the same as those in Figure 32 (d) described previously. Figure 35 (e) also shows upper-level or mid-upper-level streaks of greater intensity which resulted from the incidence of the letter "t" several places in the address.

It should be noted that the photographic paper on which the cross-correlation patterns were recorded did not encompass the entire observation plane. For this reason the extreme left-hand and right-hand portions of the resultant patterns do not appear in the cross-correlation records of Figure 35 and Figure 36.

In order to compare characteristics of handwritten material to those of hand-printed material, the same three-line address used to obtain the cross-correlation patterns of Figure 35 was hand-printed. The slope and spacing were duplicated as nearly as possible to obtain the three-line address in Figure 36. Although an effort was made to duplicate the slope of the handwriting, the subjective determination of maximum contrast corresponded to an A-plane stripe orientation of about 22 degrees. Further, there is a perceptible difference in the contrast in the cross-correlation pattern thus obtained and the pattern obtained in Figure 36 (c) for an A-plane stripe orientation of 30 degrees. There is

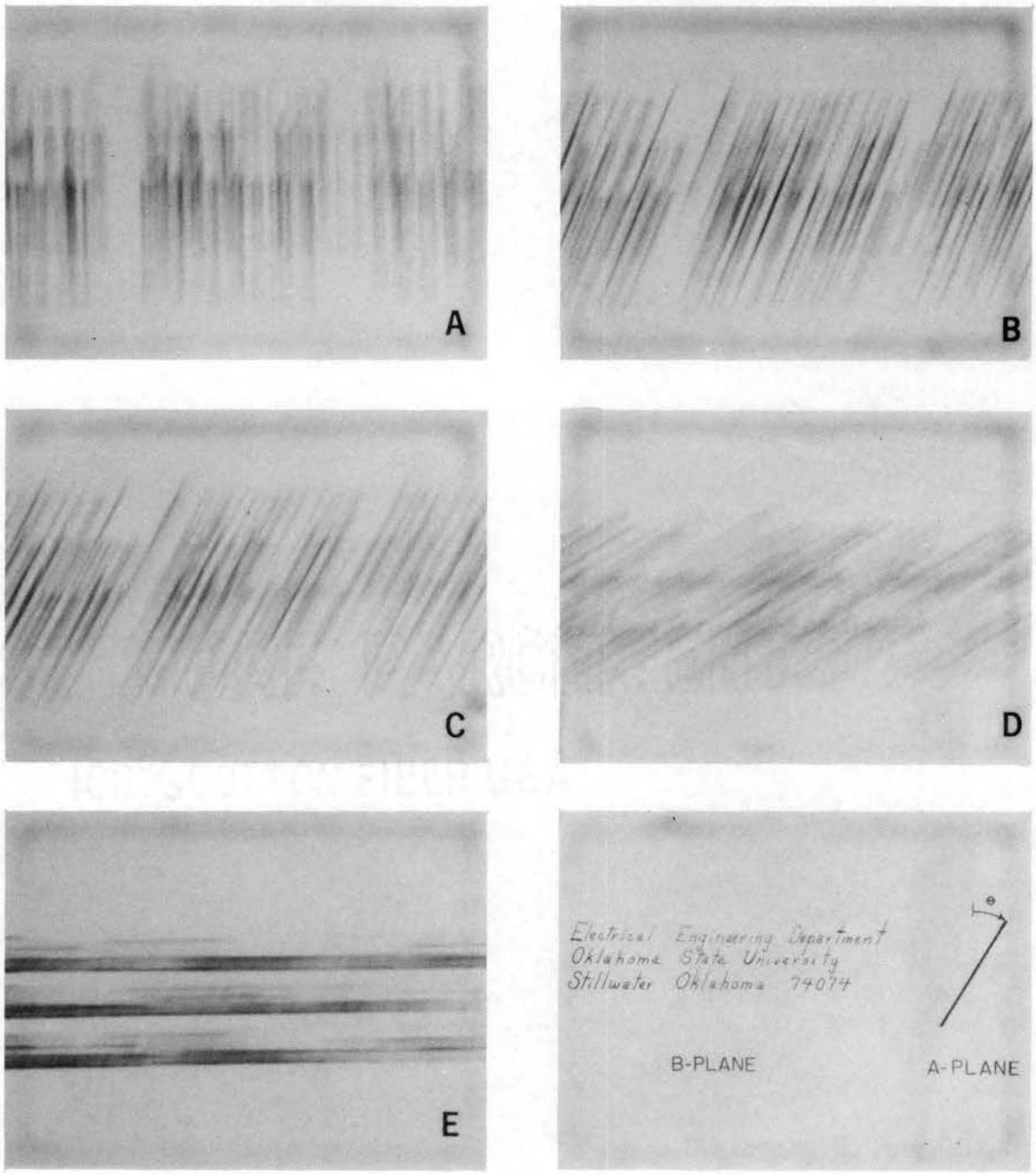

Figure 36. Cross Correlation Between a Hand-Printed Three-Line Address and a Single Narrow Stripe Inclined at (a) 0, (b) 22, (c) 30, (d) 60 and (e) 90 Degrees

also a reduction in relative intensity for the 60-degree features in the hand printing shown in Figure 36 (d) compared to the same angle for the handwriting. Although a base line characteristic is evident in Figure 36 (e) for the hand printing, it is neither as intense in an absolute sense nor as intense relative to the intermediate-level line as for the handwritten address. Significance of this and other contrasting features in the previous experiments is discussed further in the following chapter.

CHAPTER VII

DISCUSSION

It was found, as detailed in the two previous chapters, that certain features could be abstracted from two-dimensional patterns using the optical cross-correlation technique. While the scope of a study of this sort must necessarily be limited, several possibilities for application and extended study appear at this point.

Application to a Reading Machine

Although the experiments presented in the previous chapters by no means constitute a complete feature abstraction method, several of the results seem to suggest that the optical cross-correlation technique could be effectively used in the implementation of an automatic reading machine.

Early in the machine-processing of handwritten or hand-printed material a determination of predominant slant would probably be required. As noted in several of the experiments in Chapter VI, two phenomena accompanied the positioning of the single narrow stripe coincident with the dominant slant axis of the writing. The contrast of the resultant pattern was at a maximum, and further, the predominant spatial frequency of the cross-correlation pattern seemed to be at a minimum. A detection scheme for such an occurence could comprise a fixed rate scanning device and photo detector to scan perpendicularly to the narrow stripe's axis

while integrating the light intensity function along the axis of the stripe. Available electronic circuitry could then be used for detection of the maxima and minima as required.

Location of the individual lines of handwriting or hand printing could possibly be achieved by use of the horizontally oriented narrow stripe with horizontal integration of the light intensity and vertical scanning. This method of locating the individual lines would not be affected by the overlap of characters which often occurs vertically between lines of handwriting. The scanning results should also serve to make discrimination between handwriting and hand printing possible based on the comparisons between Figure 35 (e) and Figure 36 (e) mentioned in Chapter VI. Presently this discrimination seems to be a significant problem in the realization of reading machines.

Presumably, the material to be analyzed would be transferred at some point in the process by a typical video system. In this case, the individual lines of the material could be analyzed by electronic blanking of the undesired lines.

As noted previously in the experimental results, word separation is preserved when only a single line of the handwriting or hand printing is considered. This would allow for the partitioning of individual words for further analysis. In the case of handwriting, this would probably be the finest partitioning done since evidence supported by the work of Mermelstein and Eden (6) indicates that context must be considered in any automatic handwriting recognition system.

Although supporting data are not available, it seems that individual stroke spacing relative to the average spacing of strokes in handwriting might yield an invariant in the character recognition problem.

It would also seem that determination of word length in terms of average spatial period would have more significance in a recognition system than the physical dimension on the page.

Possible Extension of Studies

The facility of investigation of spatial frequency characteristics of handwritten words and similar patterns would be greatly enhanced if the size of either the A-plane or B-plane pattern was easily variable. Use of a projection cathode-ray tube in the place of the light source, diffuser and A-plane transparency would allow this variation quite readily if used in conjunction with a video signal source and a suitable raster control.

Some relative size variation could be simulated by variation of the B-plane pattern position. Size variations achieved in this way would necessarily affect both dimensions equally and would necessarily cause variation in the size of the C-plane pattern as Equation (2-4) suggests. The nature of the particular experimental laboratory equipment shown in Figure 5 precluded significant variation of the spacing between the various planes of the system. Subsequent studies should have some sort of size control, preferably a cathode-ray tube in the A plane.

Possible directions for extension of optical cross-correlation research certainly include evaluation of more refined feature abstraction techniques for handwritten script as well as similar techniques for automatic identification of spiral storm cloud patterns appearing in weather satellite photographs.

CHAPTER VIII

SUMMARY AND CONCLUSIONS

The results and conclusions of this investigation of optical cross correlation of two-dimensional patterns may be itemized as follows.

1. A survey of the literature was made to examine prior works in cross correlation of two-dimensional patterns by optical means.

2. The theory underlying the various experimental methods for obtaining two-dimensional cross correlation by optical means was examined and further developed into the form of a more concise and more rigorously defined theorem.

3. An experimental laboratory system was designed, constructed and tested in order to obtain cross-correlation functions for arbitrary experimental patterns.

4. Attention was given to the comparison of theoretical predictions to experimental cross-correlation results for simple geometric patterns. Discrepancies between theoretical and experimental results were analyzed and discussed.

5. It was found that special graphing techniques could be used advantageously to predict the basic experimental results to an acceptable order of accuracy.

6. Spatial frequency in two-dimensional patterns was found to be determinable by cross correlation with appropriate repeated patterns.

7. It was found that straight-line features could be readily

abstracted from handwriting and other two-dimensional patterns by optical cross correlation with a narrow stripe.

8. A discussion was presented which included some of the more apparent possibilities for application of the optical cross-correlation technique to a reading machine and some areas for extension of research in this area.

It is felt that these studies have shown that optical cross-correlation techniques hold considerable promise for use in implementation of two-dimensional pattern recognition systems. It is felt that research should be conducted toward refinement of feature abstraction in handwriting and subsequently toward statistical analysis of the occurence of these features in arbitrary samples of handwritten material.

BIBLIOGRAPHY

1. Rosenblatt, Frank. "Perceptron Simulation Experiments." Proceedings of the Institute of Radio Engineers, Volume 48, Number 3 (March, 1960), 301-309.

2. Widrow, Bernard and Marcian E. Hoff. "Adaptive Switching Circuits." Wescon Convention Record, Part 4 (August, 1960) 96-104.

3. Steinbuch, Von K. "Die Lernmatrix." Kybernetik, Band 1, Heft 1 (January, 1961), 36-45.

4. Bolie, Victor W. "A Cognitive Learning Program Based on Alphabets of Linearly Independent Symbols." Proceedings of the National Aerospace Electronics Conference, (May, 1965), 381-390.

5. Eden, Murray. "Handwriting and Pattern Recognition." IRE Transactions on Information Theory, Volume IT-8 (February, 1962), 160-166.

6. Mermelstein, Paul and Murray Eden. "A System for Automatic Recognition of Handwritten Words." Proceedings of the Fall Joint Computer Conference, (1964) 333-342.

7. Blackwell, H. Richard. "Neural Theories of Simple Visual Discriminations." Journal of the Optical Society of America, Volume 53, Number 1 (January, 1963), 129-160.

8. Kazmierczak, H. and K. Steinbuch. "Adaptive Systems in Pattern Recognition." IEEE Transactions on Electronic Computers, Volume EC-12 (December, 1963), 822-835.

9. Cutrona, L. J., E. N. Leith, C. J. Palermo and L. J. Porcello. "Optical Data Processing and Filtering Systems." IRE Transactions on Information Theory, Volume IT-6 (June, 1960) 386-400.

10. Montgomery, W. D. and P. W. Broome. "Spatial Filtering." Journal of the Optical Society of America, Volume 52, Number 11 (November, 1962), 1259-1275.

11. Vander Lugt, A. "Signal Detection By Complex Spatial Filtering." IEEE Transactions on Information Theory, Volume IT-10 (April, 1964), 139-145.

12. Falk, Howard. "Optical Character-Recognition Systems." Electro-Technology, (July, 1964), 42-52.

13. McLachlan, Dan. "The Role of Optics in Applying Correlation Functions to Pattern Recognition." Journal of the Optical Society of America, Volume 52, Number 4 (April, 1962), 454-459.

14. McLachlan, Dan and William R. Philips. "A Versatile Projector for Assisting in Crystal Structure Determinations." The Review of Scientific Instruments, Volume 28 (October, 1957), 793-797.

15. Kovasznay, Leslie S. G. and Ali Arman. "Optical Autocorrelation Measurement of Two-Dimensional Random Patterns." The Review of Scientific Instruments, Volume 28 (October, 1957), 793-797.

16. Meyer-Eppler, W. and G. Darius. "Two Dimensional Photographic Auto-Correlation of Pictures and Alphabet Letters." Information Theory. Ed. Colin Cherry. New York: Academic Press, 1956, pp. 34-36.

17. Gerard, R. W. and J. W. Duyff. "Information Processing in the Nervous System." Exerpta Medica Foundation ICS, Number 49, The Hague, Netherlands, Mouton and Co., 1962.

18. Wiener, N. and J. P. Schade. Nerve, Brain and Memory Models. New York: Elsevier Publishing Co., 1963.

19. Reiss, Richard F. Neural Theory and Modeling. Stanford: Stanford University Press, 1964.

20. Wiener, N. and J. P. Schade. Cybernetics of the Nervous System. New York: Elsevier Publishing Co., 1965.

21. Luxenberg, H. R. and Rudolph L. Kuehn. Display Systems Engineering. New York: McGraw-Hill, 1968, pp. 233-235.

VITA

3

Paul Norman Howell

Candidate for the Degree of

Doctor of Philosophy

Thesis: OPTICAL CROSS-CORRELATION STUDIES OF TWO-DIMENSIONAL PATTERNS

Major Field: Engineering

Biographical:

Personal data: Born near Chickasha, Oklahoma, February 17, 1936, the son of Shirley Milton and Faye R. Howell.

Education: Attended grade school in Norman and Chickasha, Oklahoma; attended high school in Okmulgee and was graduated from Chandler High School, Chandler, Oklahoma in May, 1954; received the degree of Bachelor of Science in Electrical Engineering from Oklahoma State University in May, 1959; attended University of Wisconsin part time from September, 1959 to January, 1960; attended University of Minnesota, Extension Division, part time one quarter in 1960; received the Master of Science degree with a major in Electrical Engineering from Oklahoma State University in May, 1964; completed requirements for the Doctor of Philosophy degree at Oklahoma State University in May, 1969.

Professional Experience: Student trainee-electronics engineer, Facilities Flight Inspection Section of the FAA, Summer, 1958; Systems Engineer, AC Electronics Division, General Motors Corporation, February 1959 to March 1960; evaluation engineer and design engineer, Aeronautical Division, Honeywell, Incorporated, April, 1960 to September, 1962; graduate teaching assistant, Electrical Engineering Department, Oklahoma State University, Spring, 1964; Instructor of electricity and electronics, The Technical Institute, Oklahoma State University, September, 1964 to June, 1967; graduate research and teaching assistant, Electrical Engineering Department, Oklahoma State University, June, 1968 to May, 1969.

Professional Organizations: Registered Professional Engineer in Oklahoma; Member of the Institute of Electrical and Electronic Engineers, Eta Kappa Nu, and Sigma Tau.